DOI: 10.1002/ejic.200600923

Paramagnetic (Alkene)Rh and (Alkene)Ir Complexes: Metal or Ligand Radicals?

Bas de Bruin*[a] and Dennis G. H. Hetterscheid[b]

Dedicated to Professor Karl Wieghardt on occasion of his 65th birthday

Keywords: Rhodium / Iridium / Alkene ligands / Metallo-radicals / Ligand radicals

In this review a detailed overview is given of the (electronic) structure and reactivity of open-shell (paramagnetic) alkene rhodium and iridium complexes M^x(alkene) (M = Rh, Ir; x = 0, +II). In most cases these species are highly reactive, but some notable exceptions of stable species for which not much reactivity has been described are also included (section 2). Understanding the electronic structure of the reactive nitrogen-ligand-based [M^{II}(por)(alkene)] and [M^{II}(alkene)(N-ligand)]$^{2+}$ species (section 3) is complicated by a substantial spin distribution over the metal and the alkene ligand. This dual-mode metallo-radical and ligand radical behavior is reflected by their high and diverse reactivity. Metallo-radical character is demonstrated by a variety of metal-to-radical coupling reactions with a series of other radicals, as well as metal-based allylic hydrogen atom abstractions from M^{II}(α-alkene) species. On the other hand, (donor induced) ligand radical character is crucial in a variety of M–C and C–C radical coupling reactions, C–O bond formation by oxygenation of M^{II}(alkene) species and alkene "insertions" into (por)M–H bonds. The review concludes with some speculations about possible roles of paramagnetic M(olefin) (M = Rh, Ir) species in catalytic olefin oxygenation and carbene transfer reactions.

(© Wiley-VCH Verlag GmbH & Co. KGaA, 69451 Weinheim, Germany, 2007)

1. Introduction

Our understanding of Rh and Ir organometallic chemistry is mainly based on studies of diamagnetic complexes in homogeneous solutions. Much less is known of the structure, reactivity and physical properties of their *paramagnetic* analogs. Interest in the properties and reactivity of such open-shell organometallic species is however rising.[1] This is triggered by the idea that such species might reveal special reactivity patterns, perhaps even as crucial intermediates in some catalytic reactions.[2]

[a] University of Amsterdam, Van't Hoff Institute for Molecular Chemistry (HIMS), Department of Homogeneous and Supramolecular Catalysis,
Nieuwe Achtergracht 166, 1018 WV Amsterdam, The Netherlands
Fax: +31-20-525-6422
E-mail: bdebruin@science.uva.nl
[b] Radboud University Nijmegen, Institute for Molecules and Materials (IMM),
Toernooiveld 1, 6525 ED Nijmegen, The Netherlands

Bas de Bruin obtained his PhD in 1999 from the Radboud University Nijmegen (the Netherlands). In the same year he joined the group of Prof. Karl Wieghardt at the Max-Planck Institute for Bio-Inorganic Chemistry in Mülheim/Ruhr (Germany) as an Alexander-von-Humboldt fellow. A year later he returned to the Metal-Organic Chemistry group of Prof. Anton W. Gal in Nijmegen as an assistant professor (UD). In 2005 he received a national NWO-VIDI grant to start up an independent research-line. November 2005 he moved to the University of Amsterdam (UvA) to join the Homogeneous and Supramolecular Catalysis group.

Dennis Hetterscheid obtained his master's degree in Chemistry in 2002 at the Radboud University Nijmegen (the Netherlands). Currently he is finishing his PhD at the same university (under supervision of Bas de Bruin), dealing with the synthesis, characterization and reactivity of mononucleair Rh^{II} and Ir^{II} complexes. July 2006 he obtained a national NWO-Rubicon grant for a two-year postdoc abroad, which he will carry out at the Massachusetts Institute of Technology in the group of Prof. Richard R. Schrock.

 © 2007 Wiley-VCH Verlag GmbH & Co. KGaA, Weinheim

Paramagnetic Rh and Ir species are frequently more reactive than their closed-shell counterparts, and reveal a very different reactivity. Most of these metallo-radicals are low-spin 17- or 19-VE (valence electron) species with the unpaired spin-density located *at the metal*. Consequently, most of these species reveal metal-centered radical-type reactivity like halogen-atom abstraction, hydrogen abstraction and capture of other radicals by the metal (which includes dimerization with formation of metal–metal bonds).[3] Even more reactive Rh^{II} porphyrin species are capable of breaking C–H bonds of rather inert substrates such as methane and methanol.[4] The reactivity of these "metallo-radicals" thus closely resembles that of an organic radical.

With increasing number of papers reporting about paramagnetic mononuclear Rh and Ir species,[5] their alkene adducts are still quite rare. This is not surprising, because these species tend to be very reactive and reveal a remarkable diversity of different radical-type reactions, both at the metal and at the alkene fragment.

Interestingly, the π-accepting alkene fragment is a potentially "redox non-innocent"[6] ligand (Figure 1), and "metallo-radical" and "alkene radical" descriptions both contribute to the electronic structure of a paramagnetic M^x(alkene) complex (M = Rh, Ir; x = 0, +II). Species with an increased "alkene radical" contribution generally have a stronger tendency to undergo ligand-centered radical-type reactions. Such reactions are potentially useful as new alkene functionalization reactions, very different from those in traditional organometallic chemistry. Such species might participate in (new or existing) catalytic alkene transformation reactions, such as oxygenation, cyclopropanation and other alkene functionalization reactions.

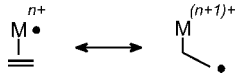

Figure 1. Ligand "redox non-innocence" in open-shell alkene transition-metal complexes.

In most cases the "metallo-radical" and "alkene radical" descriptions are limiting resonance structures of the real electronic structure, and frequently the "metallo-radical" description prevails (Figure 1). But the other extreme, in which the alkene accepts most of the spin density, can also play an important role. For example, "alkene radicals" of the type Ir^{III}–CH_2–$CH_2^{\cdot}$ are plausible intermediates in a series of radical-type reactions triggered by coordination of an additional ligand to otherwise stable Ir^{II}(ethene) species.[7,8]

In this review we provide an up-to-date overview of the unusual chemistry of paramagnetic M^x(alkene) species (M = Rh, Ir; x = 0, +II). We start with a short description of species for which not much reactivity has been reported; i.e. sterically protected species and species where spin delocalization over other parts of the molecule deprives much of the radical character of the M(alkene) fragment. This review however focuses at the intriguing reactivity of paramagnetic M(alkene) species, underlining their dual-mode "metallo-radical" and "alkene-radical" behavior.

2. M(Alkene) Species Deprived of Metal- and Alkene-Radical Behavior

In this section we summarize the properties of a few rather inert paramagnetic M(alkene) radicals (M = Rh, Ir) for which not much reactivity has been reported. This includes sterically protected species and a series of species in which the unpaired spin is highly delocalized and/or located at another part of the molecule, thus depriving much of the radical character of the M(alkene) fragment.

2.1 Highly Delocalized Radicals and Paramagnetic M(Alkene) Species Bearing the Spin Density at Other Parts of the Molecule

Compared to alkenes, some well-known other "redox non-innocent" ligands are even more inclined to accept unpaired electrons from the metal to form ligand radicals. Paramagnetic M(alkene) species containing other "redox non-inocent" ligands are less inclined to undergo metal- or alkene-centered radical reactions. The radical is usually substantially stabilized when the spin density is spread out over an extended π system of the "redox non-innocent" ligand. Delocalization of unpaired spin density over multiple metal atoms of multinuclear species and clusters is another way to stabilize open-shell M(alkene) species (M = Rh, Ir). Such examples are summarized in this section.

Spin Delocalization over Multiple Metal Atoms

Several paramagnetic organometallic clusters, multinuclear wires and dinuclear species involving platinum, palladium, rhodium and iridium have been reported, among them a number of alkene complexes. The unpaired electron of such species is usually strongly delocalized over multiple metal centers, and consequently they do not behave like reactive M(alkene) radicals. It is not our intention to give a full comprehensive overview of all paramagnetic multinuclear species here. We will restrict ourselves to a very concise description of some of these species, and then proceed with a focus on the radical-type chemistry of mononuclear M(alkene) species.

Most multinuclear paramagnetic clusters and wires are connected by metal–metal bonds, often supported by bridging ligands. Examples are the wire-like tri- and tetranuclear Rh and Ir compounds of the type $[Rh_3(\mu_3\text{-}L)_2(CO)_2(\eta_4\text{-}cod)_2]^{2+}$,[9] $[Rh_2Ir(\mu_3\text{-}OMe_2napy)_2(CO)_2(cod)_2]^{2+}$,[10] and $[M_4(\mu\text{-}PyS_2)_2(bis\text{-}alkene)_4]^{+}$ (M = Rh, Ir).[11] These "molecular wires" have the unpaired electron delocalized over multiple metal centers, suggestive of potential conducting properties of such wires. The delocalization of the unpaired spin density contributes to the relative stability of these species. Several mixed-valent dinuclear rhodium and iridium complexes of the type $[M_2]^{3+}$ and $[M_2]^{5+}$ have been reported (M = Rh, Ir). These species are formally M^{II} species bound to

 © 2007 Wiley-VCH Verlag GmbH & Co. KGaA, Weinheim

closed-shell M^{I} or M^{III} ions by metal–metal interactions. However, the actual electronic configuration of the $[Rh_2]^{5+}$ species is highly dependent on the type and number of ligands bound to the axial sites.[12–15] For example, in the complexes $[Rh(\eta^4\text{-cod})(\mu\text{-RNNNR})_2Ir(CO)_2]^+$ and $[Ir(\eta^4\text{-cod})(\mu\text{-RNNNR})_2Rh(CO)_2]^+$, the M(cod) fragment contains most of the unpaired electron density (80% and 75%, respectively).[16] This is even more drastic in case of $[I_2Rh(\mu\text{-RNNNR})_2Pd(\eta^3\text{-}C_3H_5)]^-$, which has 90% of the unpaired electron spin density located at the rhodium atom, with only 10% at palladium.[17] The steric bulk of these species likely protects these cod species from decomposing via allylic C–H activation (vide infra).

Semiquinone-Type Ligands

Catecholate/quinone-type ligands are nowadays well-known "redox non-innocent" ligands.[18] The metal quinone, $M^{I}(Q)$, metal semi-quinone, $M^{II}(SQ^{\cdot-})$, and metal catecholate, $M^{III}(Cat^{2-})$, are description of either one electronic ground state (mesomeric form) or are distinct electronic states which are in equilibrium (redox isomerism) (Figure 2).

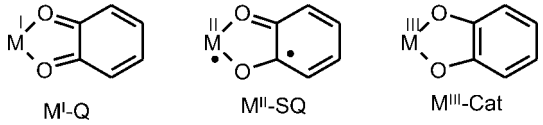

Figure 2. "Redox non-innocence" of catecholate/quinone-type ligands.

In 1992, when the "redox non-innocent" behavior of such ligands was not as well established as it is by now, formation of a paramagnetic Ir^{IV}(cod) species containing two 3,6-di-*tert*-butylcatecholate (3,6-DBCat) ligands was claimed.[19] A broad EPR resonance (200 G, g = 1.986) was observed in solution. In frozen solution, the signal splits to give a rhombic spectrum with components g_{11} = 1.948, g_{22} = 1.942 and g_{33} = 2.006, indicative of a mainly ligand-centered radical. Considering the meanwhile well-known "redox non-innocence" of catecholate/quinone-type ligands, the $[Ir^{III}$(3,6-DBCat)(3,6-DBSQ)(cod)] might thus be a better description of the electronic structure of this stable species.

Pyridine-2,6-diimine Complexes

Pyridine-2,6-diimine ligands are meanwhile also well-known to be "redox non-innocent".[20] This also seems to play a role in their Rh chemistry. Reaction of alkyl pyridine-2,6-diimine rhodium(I) complexes with dihydrogen (Figure 3) leads to the formation of a paramagnetic $[Rh^{III}(H)_2(L^{-1})]$ or $[Rh^{I}(L^{-1})(X)]$ species (X = arene solvent, dinitrogen or dihydrogen).[21] The EPR spectrum of this species in frozen toluene shows an axial signal indicative of an $S = {}^1/_2$ species [$g_{\parallel}$ = 1.9775, $g_{\perp}$ = 2.0169, $A_{\parallel}$(N) = 40 MHz] with the unpaired electron being mainly located in one of the π* orbitals of the 2,6-pyridine-diimine ligand.[21,22] The mechanism by which these species are generated is not entirely clear.

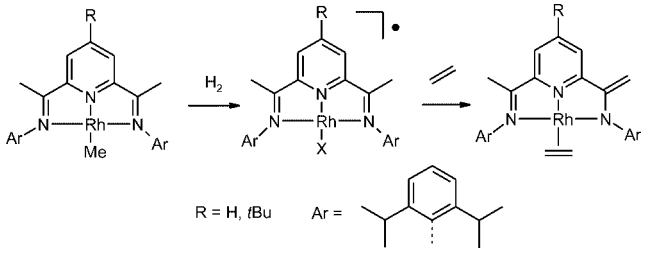

Figure 3. Chemistry of pyridine-diimine-supported alkyl rhodium(I) compounds involving open-shell intermediates.

Treatment of this species with an excess of alkenes eventually yields diamagnetic $[Rh^{I}(L_{-H})$(alkene)] species. The paramagnetic intermediate seems to be a hydrogenation catalyst of primary and secondary alkenes in the presence of H_2. The unpaired spin density in the π system of the pyridine-2,6-diimine ligand apparently has little influence on the intrinsic reactivity of Rh, as hydrogenation activity is most commonly observed for closed-shell Rh species.[21,22]

Aminyl Radical Complexes and Related Species Based on Trop-Type Ligands

The Grützmacher group has extensively used tropylidene (trop) type ligands to stabilize a series of paramagnetic rhodium and iridium complexes (Figure 4, Figure 5). Remarkably, these complexes all appear to be "ligand radicals" and/or highly delocalized radicals.

For example, trop-type ligands allow isolation of Rh^{I}-coordinated aminyl radicals. Deprotonation of cationic $[Rh^{I}(trop_2NH)(bpy)]^+$ species generates a stable (under inert atmosphere) neutral amido complex $[Rh^{I}(trop_2N^{-})(bpy)]$. Remarkably, one-electron oxidation of the latter with $[Fc]^+$ does not result in the expected Rh^{II} species, but yields an aminyl radical complex $[Rh^{I}(trop_2N^{\cdot})(bpy)]^+$ (see Figure 4). This is the first example of a stable aminyl radical coordinated to a transition metal ever reported.[23] Both detailed EPR spectroscopic investigations (g_{11} = 2.0822, g_{22} = 2.0467, g_{33} = 2.0247, A^{N}_{iso} = 45 MHz), and DFT calculations revealed that the unpaired electron is delocalized over the R_2N (ca. 57%) fragment and Rh (ca. 30%), but with a clear preference for the N atom (Figure 4, top).

The nitrogen-centered radical is stable in organic solvents for days, and even when samples are brought in contact with air or water the EPR signals persist for hours. The aminyl radical fragment nevertheless behaves as a nucleophilic radical, capable of hydrogen atom abstraction reactions from Bu_3Sn–H or RSH (R = Ph, *t*Bu, CH_2COOMe), thus regenerating the $[Rh^{I}(trop_2NH)(bpy)]^+$ starting compound and Bu_3Sn–$SnBu_3$ or RS–SR coupled products. Despite a still significant spin density at the metal, metal-centered radical reactions were not observed. In later studies

 © 2007 Wiley-VCH Verlag GmbH & Co. KGaA, Weinheim

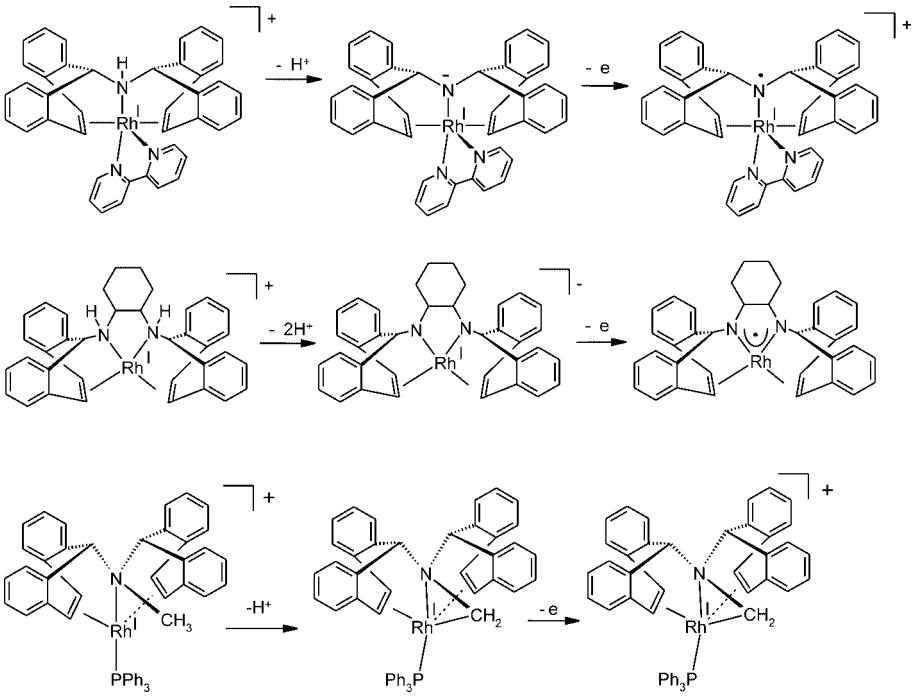

Figure 4. Top: Formation of a stable aminyl-Rh^{I} radical complex by one-electron oxidation of a amido-Rh^{I} complex. Middle: Formation of a trop-based N–M–N delocalized radical. Bottom: Formation of a highly delocalized rhoda-aza-cyclopropane radical from $trop_2N$-Me ligands.

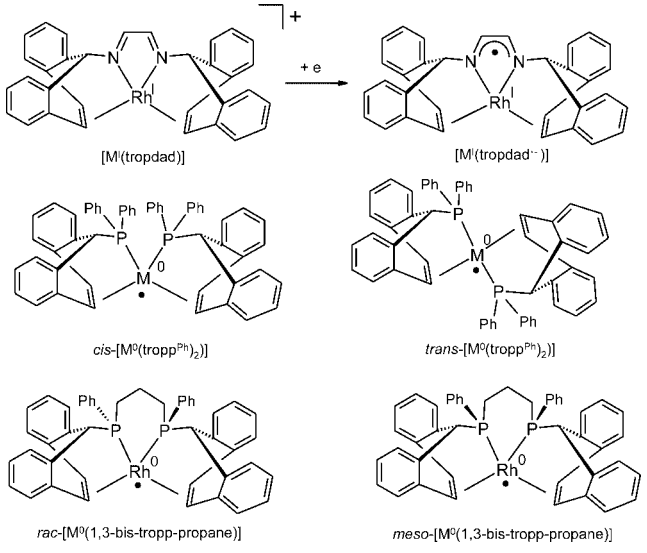

Figure 5."Low-valent" species based on the trop-type ligands.

the group also demonstrated the synthesis of a square-planar analog, in which the radical is substantially delocalized over Rh (ca. 41%) and the N atoms of two NR_2 fragments (ca. 24–28% each), see Figure 4.[24] The species still behaves as a nucleophilic *N*-centered radical, abstracting a hydrogen atom from Bu_3Si–H, despite a reduced spin localization per N atom.

Similar experiments were performed with a rhodium complex of the methyl-substituted $trop_2N$–Me ligand (Figure 4, middle). Deprotonation of $[Rh^{I}(trop_2N–Me)(PPh_3)]^+$ occurs at the methyl moiety of the $trop_2N$–Me ligand, resulting in formation of a rhoda-aza-cyclopropane ring structure.[25] The $[Rh^{I}(trop_2N–CH_2–)(PPh_3)]$ complex reveals a reversible oxidation wave in the cyclic voltammogram at a remarkably low potential (–0.51 V vs. Fc/Fc^+). Preparative one-electron oxidation of this species yields a stable cationic radical analog. The EPR data (g_{11} = 2.121, g_{22} = 2.014, g_{33} = 2.016) reveal hyperfine couplings to Rh, N, the aza-cyclopropane methylene carbon and hydrogen atoms, and the trop olefinic carbon and hydrogen atoms. DFT calculations reveal that the unpaired electron is strongly delocalized over rhodium (47%), the methylene (14%), and the four olefinic carbon atoms (15%, 15%, 3% and 3%). This species is perhaps best described as a highly delocalized radical.

"Low-Valent" Species

Tropylidene (trop) type ligands have also been used to stabilize a series of "low-valent" species. Electrochemical reduction of $[M^{I}(tropdad)]$ complexes, containing a "redox non-innocent" α-diimine fragment (Figure 5, top), leads to species in which the unpaired electron is located in the α-diimine π system.[26] Consistent with this formulation, the axial EPR spectra (M = Rh: $g_{\|}$ = 2.0113, $g_{\perp}$ = 1.9977, M = Ir: $g_{\|}$ = 2.0332, $g_{\perp}$ = 1.9870) have small deviations of the *g* values from g_e, and reveal small hyperfine couplings with Rh (no Ir hyperfine couplings were observed), and comparably stronger superhyperfine couplings with two equivalent N nuclei and two equivalent protons.

A further series of "low-valent" M(alkene) complexes were supported by tropylidene-phosphane (tropp) ligands (Figure 5). These species were also prepared by one-electron

 © 2007 Wiley-VCH Verlag GmbH & Co. KGaA, Weinheim

reduction of their M^I precursors (requiring strong reducing agents, such as metallic Li, Na or K). With the bidentate tropp^{Ph} ligands, mixtures of *cis* and *trans* isomers of [M^0(tropp^{Ph})$_2$] (M = Rh, Ir) were obtained. The EPR spectra reveal axial *g* tensors (*cis*-[(Rh^0(tropp^{Ph})$_2$]: $g_\parallel$ = 2.030, $g_\perp$ = 2.014; *trans*-[(Rh^0(tropp^{Ph})$_2$]: $g_\parallel$ = 2.050, $g_\perp$ = 2.030; *cis*-[(Ir^0(tropp^{Ph})$_2$]: $g_\parallel$ = 2.030, $g_\perp$ = 2.060; *trans*-[(Ir^0-(tropp^{Ph})$_2$]: $g_\parallel$ = 1.980, $g_\perp$ = 2.150. Detailed EPR characterization of these species reveal (super)hyperfine couplings with Rh (16–23 MHz) and the two equivalent P atoms of the tropp ligand (40–80 MHz). Remarkably, Ir hyperfine couplings were not observed, and Rh hyperfine couplings are quite small. The [(Rh^0(1,3-bis-tropp-propane)] analog (Figure 5) was prepared as a mixture of the *rac* and *meso* forms, but also in a pure *rac* form. The solution EPR spectrum of the *rac* form (g_{iso} = 2.021) reveals superhyperfine coupling with two equivalent P nuclei (84 MHz). The *meso* form (g_{iso} = 2.014) reveals superhyperfine coupling with two non-equivalent P nuclei (82 MHz and 51 MHz), likely caused by a distortion along one of the P–Rh bonds.

The *g* values of these "zero-valent" M(alkene) complexes are quite close to $g = g_e$. Their small *g* anisotropy and quite weak metal hyperfine couplings suggest that these species might not be real d^9 metal-centered radicals, but are perhaps better described as highly delocalized systems in which the unpaired spin density is substantially spread out over the metal and the trop ligand fragments. This is, however, not very clear and theoretical investigations are probably required to understand the electronic structure of these species. Spin delocalization to π-accepting CO and olefin ligands seems to be more general, and other Rh^0 complexes also reveal small deviations from $g = g_e$ (with weak metal hyperfine couplings), e.g. [Rh^0(cod)$_2$]: g_{iso} = 2.030 (A^{Rh}_{iso} not resolved);[27] [Rh^0(CO)$_4$]: g_{iso} = 2.006 (A^{Rh}_{iso} = 21 MHz).[28] The same holds for a series of Rh^0 complexes with π-accepting P ligands, which reveal larger phosphorus superhyperfine couplings than metal hyperfine couplings.[29] DFT calculations are in progress, and will hopefully lead to a more detailed understanding of the electronic structure of these Rh^0 species in the near future.[30] Notably, Rh^0 complexes of phosphinine-ring (P-analogs of pyridines, R_5C_5P) containing macrocyclic ligands (known to accommodate electrons) reveal similar EPR parameters (g_{iso} = 2.0016, A^P_{iso} = 49, A^{Rh}_{iso} not resolved; g_{iso} = 2.0180, A^P_{iso} = 271 MHz, A^{Rh}_{iso} = 27 MHz). According to DFT calculations (supported by EPR property calculations) these latter species are best described as ligand radicals.[31]

2.2 Sterically Protected Species

Sterically Protected M^0(alkene) Species

Rh^0(cot) complexes (cot = cyclooctatetraene) with the very bulky $CpPh_5^-$ ligand have been prepared electrochemically.

Electrochemical reduction of [Rh^I(CpPh$_5$)(1,5-η^4-cot)] (cot = cyclooctatetraene) initially leads to the 1,5-COT Rh^0 analog, but this species quickly converts to the more stable 1,3-cot Rh^0 isomer (Figure 6). As a consequence, reoxidation of the Rh^0(1,3-cot) species occurs at a less negative potential (–1.37 V vs. Fc/Fc$^+$, Fc/Fc$^+$ = ferrocene/ferrocenium) than reduction of the Rh^I(1,5-cot) species (ca. –2.7 V vs. Fc/Fc$^+$). The EPR spectrum of [Rh^0(CpPh$_5$)(1,3-η^4-cot)] reveals a rhombic spectrum with g_1 = 2.064, g_2 = 2.014 and g_3 = 1.893. The g_2 line reveals a resolved Rh hyperfine coupling (ca. 20 MHz). No further reactivity has been reported.

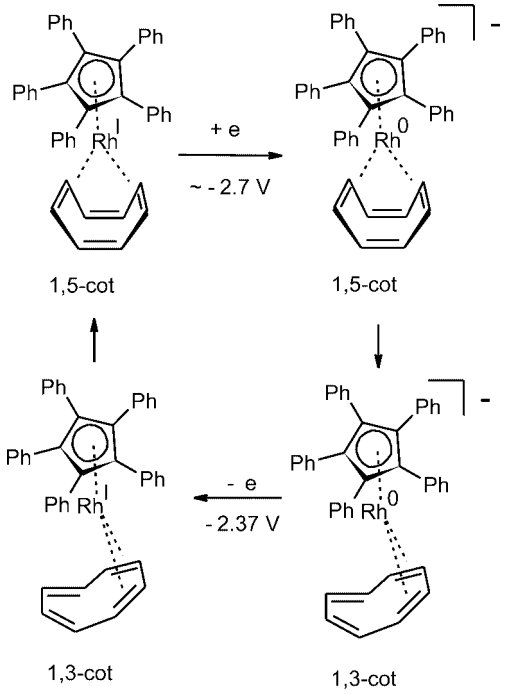

Figure 6. Formation of [Rh^0(CpPh$_5$)(1,3-η^4-cot)] upon one-electron reduction of [Rh^I(CpPh$_5$)(1,5-η^4-cot)].

Not much is known about the intrinsic reactivity of "zero-valent" M(alkene) species. Metal or alkene reactivity has not been reported for any of the above species, but this might be because these species are protected by steric bulk and/or substantial delocalization of their spin density. The situation might be different for species which are less delocalized and better accessible. This seems to be the case for [Rh^0(cod)$_2$], the only "zero-valent" species for which metal and alkene radical reactivity has been reported (to our best knowledge). [Rh^0(cod)$_2$] was prepared by electrochemical reduction of the [Rh^I(cod)$_2$]$^+$ precursor (cod = *Z,Z*-1,5-cyclooctadiene).[32] At low temperatures, the 17 VE (VE = valence electron) species is sufficiently long-lived for EPR measurements, revealing rhombic *g* values g_1 = 2.056, g_2 = 2.019 and g_3 = 2.016. Poorly resolved Rh hyperfine couplings (ca. 40–60 MHz) were observed. In chlorinated solvents such as CH_2Cl_2, the species abstracts a Cl atom from the solvent to form [{Rh^I(μ$_2$-Cl)(cod)}$_2$]. In acetone, the fate of [Rh^0(cod)$_2$] is less clear, but NMR spectroscopic data point to formation of diamagnetic species containing π-allylic moieties derived from cod, as is also observed for M^{II}(cod) species with an accessible metal center (see section 3.3).

 © 2007 Wiley-VCH Verlag GmbH & Co. KGaA, Weinheim

Sterically Protected M^{II}(alkene) Species

Most divalent M^{II}(alkene) complexes are based on hard multidentate N-donor ligands (see section 3). Exceptions are a couple of stable M^{II}-cod complexes (cod = cyclooctadiene) stabilized by very bulky σ-aryl $C_6Cl_5^-$ and pentaphenylcyclopentadienyl (η^5-$CpPh_5^-$) type ligands, namely $[Ir^{II}(C_6Cl_5)_2(cod)]$,[33] $[Rh^{II}(C_6Cl_5)_2(cod)]$,[34] $[Rh^{II}(\eta^5$-$C_5Ph_5)(1,5\text{-cod})]^+$,[35] and $[Rh^{II}(\eta^5$-$C_5Ph_5)(1,3\text{-cod})]^+$,[35] see Figure 7. Steric shielding of the metal by the bulky ligands apparently results in stable species, and these complexes can be kept in solution for many hours without decomposition.

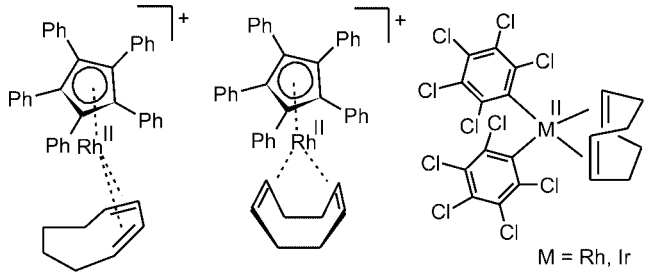

Figure 7. Stable M^{II}(alkene) complexes stabilized by η^5-$CpPh_5$ and σ-aryl-type ligands.

Rhombic EPR spectra have been observed for $[Ir^{II}(C_6Cl_5)_2(cod)]$ (g_{11} = 3.00, g_{22} = 2.79, g_{33} = 1.85) and $[Rh^{II}(C_6Cl_5)_2(cod)]$ (g_{11} = 2.55, g_{22} = 2.45, g_{33} = 1.99). The large *g* anisotropies are consistent with the proposed electronic structures, with the unpaired electron mainly residing in a d_{xy} or d_{z^2} orbital (with the *z* axis perpendicular to the coordination plane of rhodium). Substantially larger spin–orbit couplings are observed for the Ir compound (g_{av} = 2.55) than for the Rh compound (g_{av} = 2.32) which is usual for third row-compared to second-row transition metals. As expected, the $[Rh^{II}(\eta^5$-$C_5Ph_5)(1,3\text{-cod})]^+$ radical also gives rise to a rhombic EPR spectrum (g_{11} = 2.329, g_{22} = 2.120, g_{33} = 2.003). The 1,5 isomer $[Rh^{II}(\eta^5$-$C_5Ph_5)(1,5\text{-cod})]^+$ reveals an axial EPR spectrum ($g_{\|}$ = 2.181, $g_{\perp}$ = 1.997) indicative of an approximate C_{2v} symmetry. Neither of the species reveals resolved hyperfine couplings with the ^{103}Rh nucleus, preventing assignments of the orbital composition of the SOMO.

Electrochemically reversible oxidation has been reported for the related complex $[Rh^{I}(Cp)(ethene)_2]$. Coulometrically generated samples revealed a broad spectrum around *g* = 1.9855 without a resolved hyperfine structure in dimethoxyethane solution at –70 °C (frozen solutions at 20–100 K would have probably resulted in more informative spectra).[36,37] A detailed characterization of this radical cation, which is only stable at low temperatures, is lacking so far. Clearly such Cp^- complexes are much less stable than the above sterically protected $CpPh_5^-$ species.

More information about the intrinsic reactivity of M^{II}(alkene) species has been gathered using N-ligands. This is described in section 3.

3. Reactive M^{II}(alkene)(N-ligand) Species. Metal or Alkene Radicals?

Apart from the above exceptions, all other M^{II}(alkene) complexes (M = Rh, Ir), and reactions of M^{II} radicals with alkenes, have been studied using mononuclear complexes with multidenate N-donor ligands. Neutral-type complexes of the $[M^{II}(por)]$-type based on dianionic porphyrinato (por^{2-}) ligands and dicationic complexes of the type $M^{II}(N_4\text{-ligand})]^{2+}$ and $[M^{II}(N_3\text{-ligand})]^{2+}$ based on neutral, podal $N\{CH_2Py\}_n$ (*n* = 2, 3) type ligands have so far dominated these studies (Figure 8).

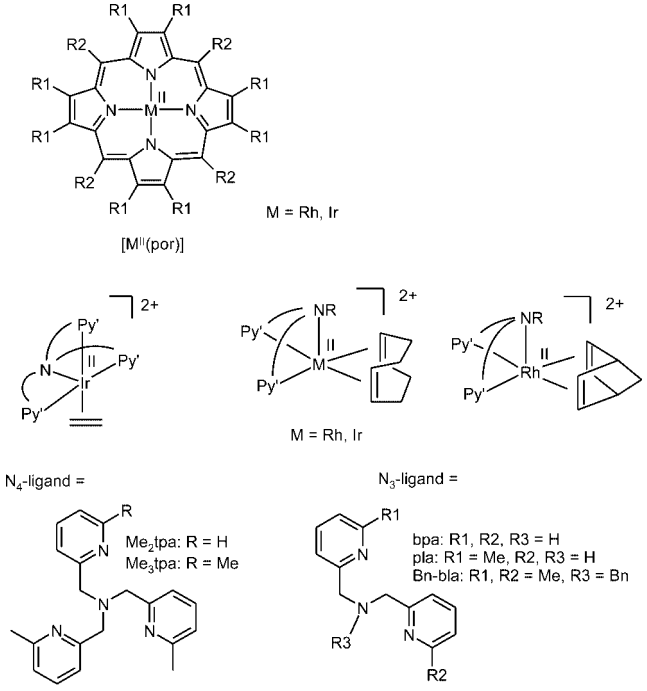

Figure 8. Structure of neutral $[M^{II}(por)]$ and dicationic $[Ir^{II}(N_4\text{-ligand})(ethene)]^{2+}$, $[Rh^{II}(N_3\text{-ligand})(nbd)]^{2+}$ and $[M^{II}(N_3\text{-ligand})(cod)]^{2+}$ species.

3.1 Geometries and Electronic Structures

Before we continue with a more detailed description of the geometry and electronic structures of complexes of the type $[M^{II}(por)]$ and $[M^{II}(N\{CH_2Py\}_n)]^{2+}$ (*n* = 2, 3) (section 3.1.2 and 3.1.3), let us first consider the most important differences between these types of species which are most relevant for their reactivity.

3.1.1 Metal or Ligand Radicals?

First of all, the porphyrinato complexes have *trans* vacant sites, and although perhaps not entirely impossible, *cis* reactivity patterns of alkenes and other substrates are not very likely for $[M^{II}(por)(alkene)]$ species. This should not be a problem for the dicationic $[M^{II}(alkene)(N_4\text{-ligand})]^{2+}$ and $[M^{II}(bis\text{-alkene})(N_3\text{-ligand})]^{2+}$ species, having a "vacant site" *cis* to the alkene (half occupied by the unpaired electron). Alkenes have a low affinity for $[M^{II}(por)]$ radicals, and once formed such alkene adducts tend to be very reac-

 © 2007 Wiley-VCH Verlag GmbH & Co. KGaA, Weinheim

tive. As a result, alkene adducts of $[M^{II}(por)]$ radicals cannot be isolated, although they do reveal interesting reactions towards alkenes (section 3.2.1–3.3). Alkenes bind much stronger to dicationic $[M^{II}(N_4\text{-ligand})]^{2+}$- and $[M^{II}(N_3\text{-ligand})]^{2+}$-type complexes, allowing isolation and detailed characterization of the alkene adducts (section 3.1.2).

For the neutral $[M^{II}(por)]$ species, alkene→metal σ bonding is expected to be weaker than the dicationic $[M^{II}(N_4\text{-ligand})]^{2+}$ and $[M^{II}(N_3\text{-ligand})]^{2+}$ complexes (Figure 8). On the other hand, metal→alkene π(back)bonding, which contributes substantially to the metal–alkene interaction (Chatt–Dewar–Duncanson model), is expected to be stronger for the neutral $[M^{II}(por)]$ species. Therefore, one cannot ascribe the different alkene affinities *only* to the charge differences.

Another important difference between these types of complexes is the orbital symmetry. The $[M^{II}(N_4\text{-ligand})]^{2+}$ and $[M^{II}(N_3\text{-ligand})]^{2+}$ complexes have an empty $d_{x^2-y^2}$ and an empty p orbital available for alkene→metal σ bonding. The planar $[M^{II}(por)]$ species, however, have the *half-filled* d_{z^2} orbital and the higher lying empty p orbital available for alkene→metal σ bonding, further weakening this interaction (Figure 9). A consequence of the d_{z^2} orbital being involved in binding of the alkene in 17-VE $[M^{II}(por)(alkene)]$ species is that the alkene ligand will always bear a significant part of the unpaired spin density, thus making the alkene fragment sensitive to radical reactions. This is clearly reflected by the reactivity of $[M^{II}(por)(alkene)]$ species (see sections 3.2–3.3).

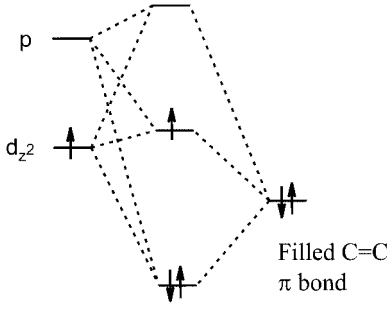

Figure 9. Alkene→metal σ bonding in $[M^{II}(por)(alkene)]$ species.

The alkene ligands of the 17-VE dicationic $[M^{II}(alkene)(N_4\text{-ligand})]^{2+}$ and $[M^{II}(di\text{-alkene})(N_3\text{-ligand})]^{2+}$ complexes do not bear much spin density (< 5%). The d_{z^2} orbital, in which the unpaired electron is located, predominantly interacts with N_{amine} donors, leaving the alkene ligands virtually unaffected.

Donor-Induced Metal to Ligand Radical Transformations in "19-VE" Species

Binding of a 6th ligand to 17-VE five-coordinate M^{II}-(alkene) species substantially influences the reactivity of these species. Binding of an additional σ-donor ligand without loss of the alkene should be more easy for the dicationic $[M^{II}(alkene)(N_4\text{-ligand})]^{2+}$ and $[M^{II}(bis\text{-alkene})(N_3\text{-ligand})]^{2+}$ complexes compared to the neutral $[M^{II}(por)(alkene)]$ species. Indeed, indications for formation of such 19-VE intermediates have thus far only been obtained for $[Ir^{II}(ethene)(Me_ntpa)]^{2+}$ (n = 2, 3) complexes.

Although the PyMe groups shield the "vacant site" of $[Ir^{II}(Me_ntpa)(ethene)]^{2+}$ species (n = 2, 3) from attack by bulky reagents, MeCN is small enough to coordinate to iridium *trans* to the amine (Figure 10). Obviously, this is most easy for the least hindered Me_2tpa species (n = 2). Binding of MeCN (or other small ligands) causes these otherwise inert species to undergo alkene radical reactions (see sections 3.2.1 and 4).

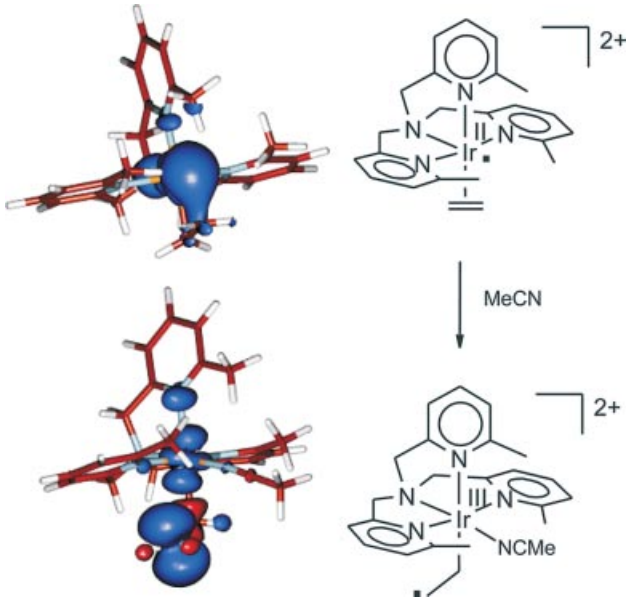

Figure 10. Spin density plots of $[Ir^{II}(Me_3tpa)(CH_2{=}CH_2)]^{2+}$ (above) and $[Ir^{III}(\text{-}CH_2\text{-}CH_2^{\cdot})(Me_3tpa)(NCMe)]^{2+}$ (below).

According to DFT calculations, these MeCN adducts have the ethene fragment coordinated in a "slipped" way. Whereas the α-carbon of the "slipped alkene" fragment seems to be tetrahedral and sp^3-hybridized, the β-carbon atom is planar and sp^2-hydridized. A spin-density plot (Figure 10) reveals that these species are not real 19 VE species, but are intermediate between a 19 VE "slipped alkene" description $Ir^{II}\text{–}CH_2\text{–}CH_2^+$ and an 18 VE ethyl radical description $Ir^{III}\text{–}CH_2\text{–}CH_2^{\cdot}$, but the 18 VE ethyl radical description prevails.[7] Thus, MeCN binding apparently leads to a donor induced shift of the spin density from the metal to the alkene with formation of $Ir^{III}\text{–}CH_2\text{–}CH_2^{\cdot}$ radicals. This substantially influences the reactivity of these species (see sections 3.2.1 and 4), and constitutes a new approach to tuning the reactivity of open-shell metal-alkene complexes.

3.1.2 (Electronic) Structure of Dicationic 17-VE M^{II}(alkene)(N{CH_2Py}$_n$) Radicals

Species of the type $[Ir^{II}(N_4\text{-ligand})(ethene)]^{2+}$,[7,38,39] $[Rh^{II}(N_3\text{-ligand})(nbd)]^{2+}$[40] (nbd = norbornadiene) and $[M^{II}(N_3\text{-ligand})(cod)]^{2+}$[41,42] have been obtained from their

 © 2007 Wiley-VCH Verlag GmbH & Co. KGaA, Weinheim

M^I precursors by one-electron oxidation using either $[Fc]^+$ or Ag^+ as an oxidant (Figure 8).

Cyclic voltammograms of these complexes revealed reversible waves for the M^I/M^{II} couple in all cases, except for some of the less bulky cyclooctadiene complexes. The M^{II}/M^{III} couple was not observed at potentials below oxidation of the solvent. Direct electron-transfer (ET) disproportionation of the dicationic M^{II} species to monocationic M^I and tricationic M^{III} species is substantially endergonic (> 92–125 kJ mol^{-1} in both acetone and CH_2Cl_2), and thus an unlikely decomposition pathway of these species.

The X-ray structures of $[Ir^{II}(Me_3tpa)(ethene)]^{2+}$[7,38] and $[Rh^{II}(Bn\text{-}bla)(cod)]^{2+}$[42] as well as their M^I precursors have been reported. The M^I species adopt a trigonal-bipyramidal geometry. Upon oxidation the geometry changes to a square pyramid with the amine at the apical position and the alkene(s) and the pyridines coordinating in the basal plane. The pyridylmethyl groups shield the "vacant position" *trans* to the amine (Figure 11). On going from M^I to M^{II}, the M→alkene π backbonding becomes weaker, resulting in longer M–C and shorter C=C bonds. The M–N interactions become stronger. The structures elucidated by X-ray diffraction are consistent with DFT calculations and EPR data.

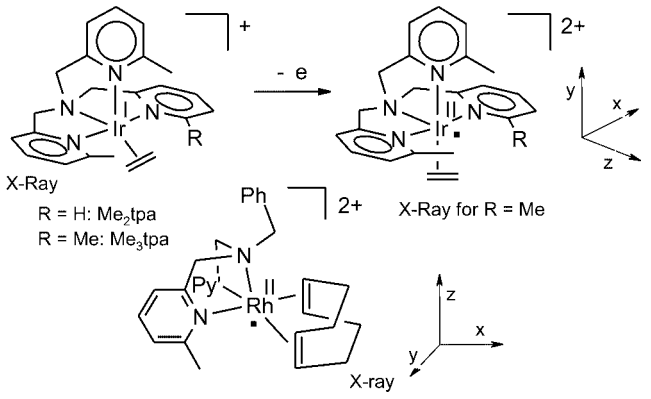

Figure 11. Sterically protected $[Ir^{II}(Me_ntpa)(ethene)]^{2+}$ and $[Rh^{II}(Bn\text{-}bla)(cod)]^{2+}$ species.

$[Rh^{II}(N_3\text{-ligand})(nbd)]^{2+}$ and $[Rh^{II}(N_3\text{-ligand})(cod)]^{2+}$ show EPR spectra with g_x, $g_y > 2$ and $g_z \approx 2$, with g_z revealing a strong (super)hyperfine coupling with both the metal and the apical N_{amine} donor.[40–42] These data suggest that the unpaired electron resides in the d_{z^2} orbital, in good agreement with results from DFT calculations. For all analogous Ir compounds the g_z value is notably lower than g_e, pointing to some mixing of the d_{z^2} orbital with a $d_{x^2-y^2}$ orbital (d_{xy} for the cod complexes) in the SOMO.

The EPR parameters calculated with DFT are in satisfactory agreement with the experimentally derived parameters. Experimental ENDOR measurements, as well as DFT spin density plots reveal that the spin density is substantially delocalized over the N_{amine} donor (15–18%) and the metal (73–78%).[42] Delocalization of the unpaired electron over the metal and the amine might contribute to the relative stability of these species.

3.1.3 (Electronic) Structure of Neutral 17-VE M^{II}(alkene)(por) Radicals

Radical-type chemistry of neutral square-planar N_4-ligand Rh^{II} species has been mainly studied with porphyrinato (por^{2-}) ligands, but similar chemistry for the dianionic planar coordinating N_4-ligands TMTAA,[43] OETAP,[44] and DBPB[45] (Figure 12) has been reported.

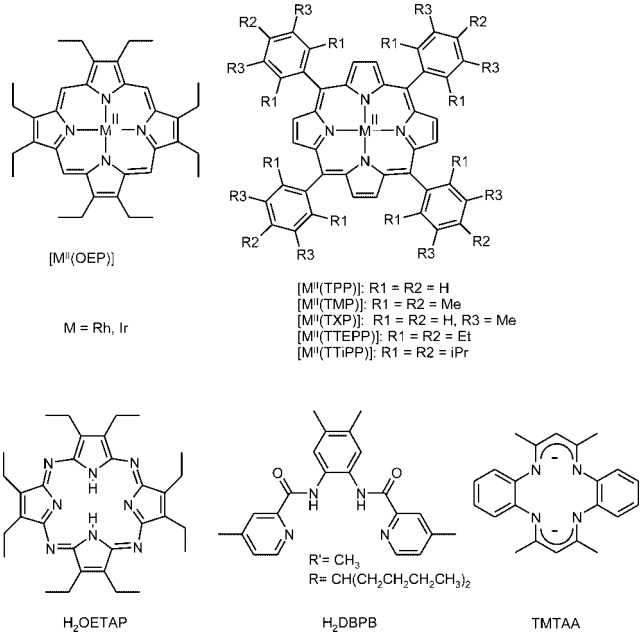

Figure 12. Porphyrinato Rh^{II} and Ir^{II} complexes and related N-ligands used in the organometallic chemistry of planar Rh^{II} metallo-radicals.

Generally, mononuclear $[M^{II}(por)]$ species (Figure 12) are prepared by thermally or photo-chemically induced homolytic M–M, M–H or M–C bond splitting of their corresponding M–M, M^{III}–Me or M^{III}–H precursors.[46] Occasionally, also (electro)chemical reduction or oxidation has been applied.[47–49]

In all cases the mononuclear square planar d^7 complexes are very reactive. As a result, the least hindered complexes containing the porphyrins OEP (octaethylporphyrinato), TPP tetraphenylporphyrinato, TTP (tetratolylporphyrinato) and TXP [tetrakis(3,5-dimethylphenyl)porphyrinato] easily dimerize (Figure 13) to form diamagnetic metal–metal-bonded dinuclear species (in which a description as M^I–M^{III} is indistinguishable from a antiferromagnetically coupled M^{II}–M^{II} system). The Rh–Rh bond is, however, rather weak and allows thermal homolytic Rh–Rh bond splitting to study the reactivity of the mononuclear species. To promote dissociation of the dinuclear Rh–Rh species in mononuclear square planar d^7 species, porphyrin ligands have been supplied with bulky groups at their periphery. The steric bulk of the porphyrin dianion decreases in the order TTiPP > TTEPP > TMP > TXP > TTP > TPP > OEP

 © 2007 Wiley-VCH Verlag GmbH & Co. KGaA, Weinheim

(see Figure 12). More bulky porphyrins result in weaker Rh–Rh bonds (Rh–Rh bond dissociation enthalpies: OEP: 69 kJ mol^{-1}; TXP: about 50 kJ mol^{-1}; TMP: about 0 kJ mol^{-1}) and consequently more reactive systems.[50–52]

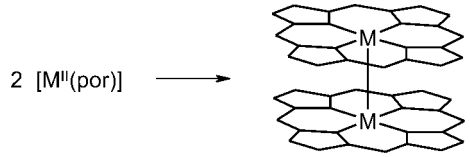

Figure 13. Formation of dinuclear M–M bonded species from [M^{II}(por)] species (M = Rh, Ir).

The complexes [Rh^{II}(TMP)], [Rh^{II}(TTEPP)], [Rh^{II}-(TTiPP)], [Ir^{II}(TTEPP)] and [Ir^{II}(TTiPP)] are sufficiently bulky to completely prevent dimerization [TMP = tetramesitylporphyrinato; TTEPP = tetra(2,4,6-triethylphenyl)porphyrinato TTiPP = tetra(2,4,6-triisopropylphenyl)porphyrinato]. EPR spectroscopy, ^{1}H NMR paramagnetic shifts and line broadening studies have proven useful to study the (electronic) structure of these paramagnetic complexes (and their adducts with ethene, see below).[52–54] EPR parameters of the rhodium complexes [Rh^{II}(TMP)] and [Rh^{II}-(TTiPP)] are consistent with a prevalent d_{z^2} SOMO associated with a $(d_{xy})^2(d_{xz,yz})^4(d_{z^2})^1$ ground state. Remarkably, the iridium complex [Ir^{II}(TTiPP)] does not reveal an observable EPR spectrum, which was explained by the presence of one or more excited states with energies close to the ground state, causing rapid electron-spin relaxation.[55] This was further confirmed by the thermal behavior of the pyrrole chemical shifts. While a linear dependence of the paramagnetic shift of [Rh^{II}(TTiPP)] against 1/T (inverse of the temperature) indicates a simple Curie paramagnetic behavior associated with a single contributing state [$(d_{z^2})^1$], the curvature of the plot for [Ir^{II}(TTiPP)] suggests that several states are thermally populated. The upfield chemical shifts of the pyrrole hydrogen atoms (δ_{pyr} = –20.9 ppm) compared to the downfield chemical shift of [Rh^{II}(TTiPP)] (δ_{pyr} = +17.5 ppm) was taken as evidence for spin population of the porphyrin π*-orbitals in case of iridium. This can be explained by assuming an $(d_{xy})^2(d_{z^2})^2(d_{xz,yz})^3$ground state, in contrast to the $(d_{xy})^2(d_{xz,yz})^4(d_{z^2})^1$ ground state observed for the rhodium analog.

3.2 Reactivity of M^{II}(alkene)(N-ligand) Species without Allylic Hydrogen Atoms

3.2.1 M–C and C–C Coupling Reactions

A variety of alkenes react with [Rh^{II}(OEP)] (Figure 12) to form binuclear alkyl-bridged [Rh^{III}(OEP)(μ-CH$_2$CHR-)-Rh^{III}(OEP)] complexes (Figure 14). The reaction of [Rh^{II}-(OEP)] with styrene was claimed to proceed by a radical chain mechanism.[56] In the absence of [Rh^{III}(OEP)(H)], the initially formed [Rh^{II}(OEP)(CH$_2$=CHPh)] intermediate reacts with another [Rh^{II}(OEP)]$_2$ complex abstracting a [Rh^{II}(por)] radical, thus yielding the alkyl-bridged species [Rh^{III}(OEP)(μ$_2$-CH$_2$CHPh-)Rh^{III}(OEP)]. In the presence of [Rh^{III}(OEP)(H)], the intermediate [Rh^{II}(OEP)(CH$_2$=CHPh)] abstracts a hydrogen atom from [Rh^{III}(OEP)(H)] to form a mononuclear alkyl complex [Rh^{III}(OEP)(CH$_2$CH$_2$Ph)] (Figure 14).

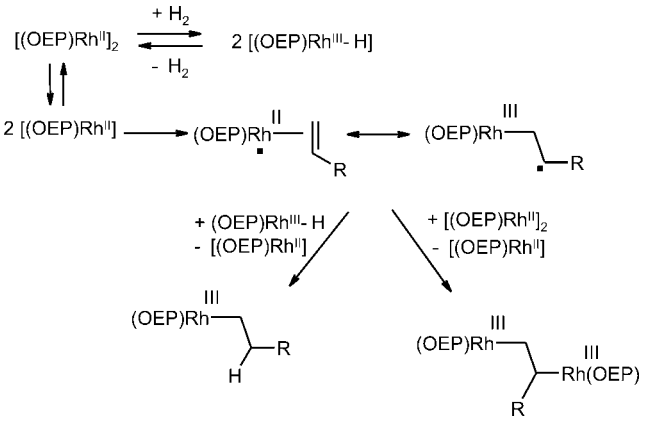

Figure 14. Reactivity of [Rh^{II}(por)] and [Rh^{III}(por)(H)] towards alkenes without allylic hydrogen atoms.

Other alkenes like acrylates[57] give similar alkyl-bridged species [Rh^{III}(OEP)(μ$_2$-CH$_2$CHR-)Rh^{III}(OEP)], and acetylenes give the corresponding μ$_2$-CH=CR-bridged species [Rh^{III}(OEP)(μ$_2$-CH=CHR-)Rh^{III}(OEP)].[58]

A series of more hindered [Rh^{II}(por)] complexes with por = TMP, TTEPP and TTiPP provide further insight in the behavior of the [Rh^{II}(por)(alkene)] intermediates. Like [Rh^{II}(OEP)], the least hindered [Rh^{II}(TMP)] reacts with ethene to form the diamagnetic ethylene-bridged species [Rh^{III}(TMP)(μ$_2$-C$_2$H$_4$-)Rh^{III}(TMP)] by a bimolecular M–C coupling reaction.[59] Increasing the steric bulk by using TTEPP prevents direct M–C coupling, and [Rh^{II}(TTEPP)] reacts with ethene via a bimolecular C–C coupling between two rhodium–ethene radicals to form the butylene-bridged species [Rh^{III}(TTEPP){μ$_2$-CH$_2$CH$_2$–CH$_2$CH$_2$–Rh^{III}-

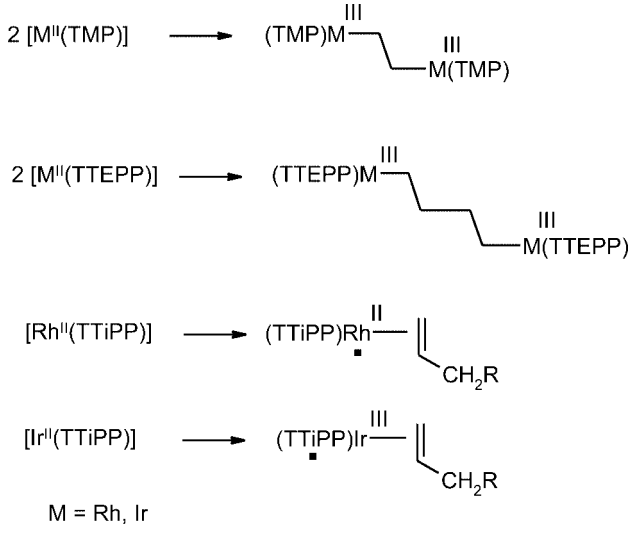

Figure 15. The reactivity of [M^{II}(por)] species changes from M–C to C–C coupling to no coupling at all upon increasing the steric bulk.

 © 2007 Wiley-VCH Verlag GmbH & Co. KGaA, Weinheim

(TTEPP)}], see Figure 15.[60] A similar intermolecular C_{alkene}–C_{alkene} bond formation involving two cot ligands was observed following oxidation of [Rh^{I}(Cp)(cot)].[61]

Neither for [Rh^{II}(TMP)] nor for [Rh^{II}(TTEPP)] any intermediates were observed with EPR spectroscopy. However, a further increase of the steric bulk by using [Rh^{II}(TTiPP)] gives rise to a reasonably stable paramagnetic ethene adduct [Rh^{II}(TTiPP)(CH_2=CH_2)]$^{\cdot}$, revealing a rhombic EPR spectrum at 90 K (g values: g_1 = 2.323, g_2 = 2.222 and g_3 = 1.982). A substantial spin population at ethene (ca. 0.29) was derived from the ^{13}C hyperfine couplings of [Rh^{II}(TTiPP)($^{13}CH_2$=$^{13}CH_2$)] (A_{zz}: 38 MHz, A_{xx} = A_{yy} ≈ 5 MHz).[60,62] The spin population at rhodium was estimated at about 0.67. The equivalence of the two ^{13}C atoms in the EPR spectrum reveals a symmetrically bound ethene π complex, and the delocalization of the unpaired electron to the ethene fragment (29%) occurs almost entirely by the C_{2p} orbitals. At temperatures > 200 K [Rh^{II}(TTiPP)(ethene)] loses the ethene fragment to form [Rh^{II}(TTiPP)].[63]

Reactions of the iridium complexes [Ir^{II}(TMP)] and [Ir^{II}(TTEPP)] with ethene proceed analogously to the above described rhodium analogs (Figure 16).[64] Like its rhodium analog, reaction of [Ir^{II}(TTiPP)] with ethene does not result in M–C or C–C coupling, and formation of the ethene adduct is witnessed by NMR, UV/Vis (λ_{max} = 444 nm and 730 nm) and EPR spectroscopy [$<g>$ = 1.987 (290 K); $g_{\|}$ = 1.96, $g_{\perp}$ = 1.998 (90 K)]. However, these spectroscopic data are indicative of a donor-induced intramolecular electron transfer from the Ir^{II} center to the porphyrin ligand π* orbital to yield a Ir^{III}(por$^{\cdot 3-}$) species. This contrasts the results obtained by ethene binding to [Rh^{II}(TTiPP)], where the unpaired electron remains in the d_{z^2} orbital.

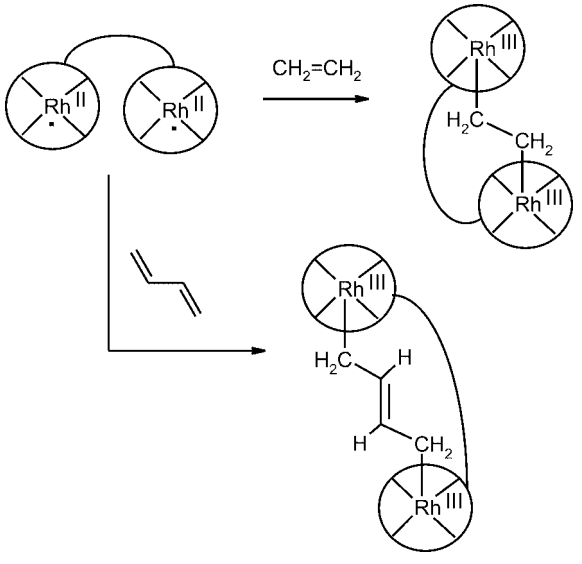

Figure 16. Reaction of alkenes with tethered (por)Rh^{II} complexes.

Selective binding of ethene and butadiene between the two rhodium sites of a tethered bimolecular bis(por)Rh species with steric demands comparable to TMP, results in selective intramolecular coupling (Figure 16).[65] This gives further support to the idea that formation of alkyl-bridged species from alkenes and [M^{II}(por)] requires a concerted action of two metallo-radical sites.[60]

The reactions of [Rh^{II}(por)] with alkenes reveal that the [Rh^{II}(por)(alkene)] intermediates have a substantial spin density at the alkene fragment. This prompted the Wayland group to investigate attempts to initiate radical polymerization of acrylates with these species.[57] Although photo-promoted radical initiation (involving homolytic Rh–C bond splitting) was achieved, direct radical initiation with [Rh^{II}(OEP)] or [Rh^{II}(TMP)] proved not possible.

On the basis of an estimated Rh–CH_2R bond dissociation enthalpy (BDE) of ca. 209 kJ mol^{-1}, the energy associated with alkene binding to [Rh^{II}(por)] estimated at 0–33 kJ mol^{-1},[57,63] and the energy required to convert ethene into its diradical $^{\cdot}CH_2$–$CH_2^{\cdot}$ (268 kJ mol^{-1}), formation of an intermediate [Rh^{III}(por)(CH_2–$CH_2^{\cdot}$)] species with 100% spin population at the β-carbon atom requires about 59 kJ mol^{-1}. Relaxation of this species to the more stable π complex [Rh^{II}(por)(CH_2=CH_2)] should be exothermic by about 59–92 kJ mol^{-1}.[57] On the basis of these arguments (and the above EPR results), the authors argued that [Rh^{II}(por)(alkene)] complexes are not authentic alkyl radicals and therefore cannot initiate alkene polymerization reactions (Figure 17).

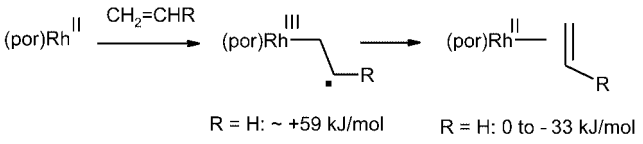

Figure 17. [Rh^{II}(por)(alkenes)]; metal- or carbon-centered radicals?

These arguments also imply that formation of "slipped olefin"/ethyl radical species [M^{II}(por)(CH_2–$CH_2^{\cdot}$)] could be rather unfavorable for these complexes. On the other hand, coupling of two [M^{II}(por)(alkene)] species with C–C bond formation to yield M^{III}–CH_2CH_2–CH_2CH_2–M^{III} are most likely to proceed via species having at least some [Rh^{III}(por)(CH_2–$CH_2^{\cdot}$)] contribution to their electronic structure. Furthermore, substituents known to stabilize radicals should favor the [Rh^{III}(por)(CH_2–$CHR^{\cdot}$)] contribution [e.g. R = Ph, C(O)R, CN, alkyls in Figure 17].

Binding of an additional σ-donor ligand to neutral 17-VE [M^{II}(por)(alkene)] species might not be very easy, but might nevertheless facilitate formation of such bent [Rh^{III}(por)(CH_2–$CH_2^{\cdot}$)] intermediates. This is inspired by recent investigations concerning the reactivity of [Ir^{II}(Me_3tpa)(ethene)]$^{2+}$ with a variation of substrates in MeCN as a solvent. Unlike the [M^{II}(por)(alkene)] species, these [Ir^{II}(Me_3tpa)(ethene)]$^{2+}$ complexes do not spontaneously form butylene or ethylene-bridged dinuclear M^{III}–CH_2-$CH_2CH_2CH_2$–M^{III} or M^{III}–CH_2CH_2–M^{III} species. In the presence of MeCN, however, such reactivity is triggered (Figure 18). These reactions likely proceed via the Ir^{III}–CH_2–$CH_2^{\cdot}$-type radicals shown in Figure 10 (see section 3.1.1). A stronger M–C bond of Ir compared to Rh is per-

 © 2007 Wiley-VCH Verlag GmbH & Co. KGaA, Weinheim

haps a further contributing factor to stabilization of the bent alkene structure in $[Ir^{III}(Me_3tpa)(MeCN)(CH_2–CH_2^{\cdot})]^{2+}$ compared to $[Rh^{II}(por)(alkene)]$.

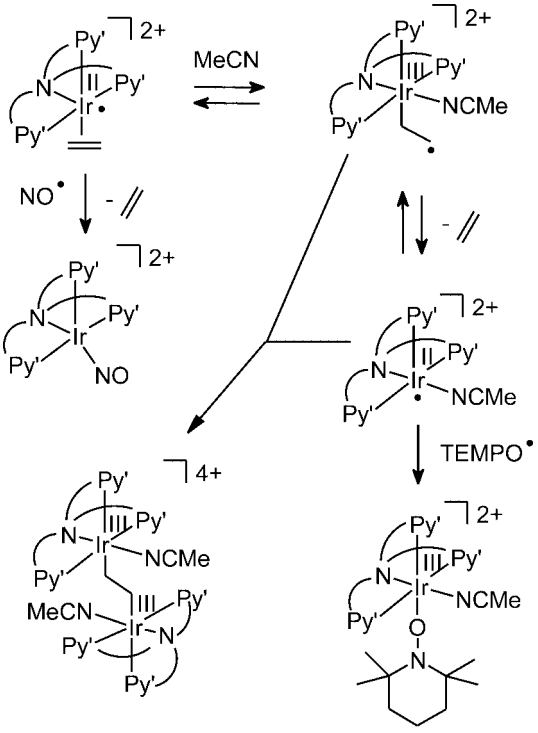

Figure 18. Formation of $Ir^{III}–CH_2CH_2–Ir^{III}$ and Ir^{III}-TEMPO via $Ir^{III}(CH_2CH_2^{\cdot})$(NCMe) and Ir^{II}(NCMe) species.

Dissociation of ethene from $[Ir^{III}(CH_2CH_2^{\cdot})(Me_3tpa)(NCMe)]^{2+}$ leads to the reactive metallo-radical $[Ir^{II}(Me_3tpa)(NCMe)]^{2+}$. This species contains only N-donor ligands and has its unpaired electron located in an orbital which is not sterically shielded by the ligand bulk. Although there is no spectroscopic evidence for formation of $[Ir^{III}(CH_2CH_2^{\cdot})(Me_3tpa)(NCMe)]^{2+}$ nor $[Ir^{II}(Me_3tpa)(NCMe)]^{2+}$, their existence can be rationalized from the reaction products of the Ir^{II}(ethene) species in acetonitrile. In the presence of the stable radical TEMPO, radical coupling of the metallo-radical $[Ir^{II}(Me_3tpa)(NCMe)]^{2+}$ with TEMPO takes place, leading to the formation of $[Ir^{III}(TEMPO^{-})(Me_3tpa)(NCMe)]^{2+}$. In the absence of TEMPO, $[Ir^{II}(Me_3tpa)(NCMe)]^{2+}$ couples with $[Ir^{II}(Me_3tpa)(CH_2CH_2)]^{2+}$, or perhaps more likely $[Ir^{III}(CH_2CH_2^{\cdot})(Me_3tpa)(MeCN)]^{2+}$ to form an ethylene-bridged species (Figure 18).[7,39] The increased reactivity on going from Me_3tpa to the less bulky Me_2tpa complex in formation of the ethylene-bridged species, is in good agreement with the proposed associative addition of acetonitrile to $[Ir^{II}(Me_ntpa)(ethene)]^{2+}$ being the first step of the dimerization process.

In contrast to reactions of $[M^{II}(por)]$ with alkenes, no butylene-bridged species were formed. Apparently, the concentration of $[Ir^{III}(CH_2CH_2^{\cdot})(N_4\text{-ligand})(MeCN)]^{2+}$ is too low for carbon–carbon coupling reactions to take place, and metal–carbon couplings with $[Ir^{II}(N_4\text{-ligand})(NCMe)]^{2+}$ species prevail.

The formation of the similar products $[\{Ir^{III}(Me_3tpa)(NCMe)\}_2(\mu_2\text{-}CH_2CH_2)]^{4+}$, $[\{Ir^{III}(Me_3tpa)(NCPh)\}_2(\mu_2\text{-}CH_2CH_2)]^{4+}$ and $[\{Ir^{III}(Cl)(Me_3tpa)\}_2(\mu_2\text{-}CH_2CH_2)]^{2+}$ indicate that this chemistry is not restricted to acetonitrile and expands to other σ-donors (nitrils, Cl^{-}, H_2O).[7,8]

3.2.2 [Rh^{II}(por)(alkene)] Intermediates in Alkene Insertions into Rh–H Bonds

Insertion reactions of alkenes into the Rh–H bonds of the less hindered porphyrinato complexes $[Rh^{III}(OEP)(H)]$ and $[Rh^{III}(TPP)(H)]$ are strongly related to the above described reactivity of $[M^{II}(por)]$ radicals with alkenes. Because $[Rh^{III}(por)(H)]$ species lack any *cis* vacant sites, these insertion reactions are quite remarkable and do not likely proceed via a common (migratory) insertion requiring coordination of the olefinic substrates *cis* to the Rh–H bond. In fact the insertion reactions are reported to proceed through radical mechanisms. The hydride species are in equilibrium with the $[Rh^{II}(por)]_2$ dimeric species (Figure 14) through bimolecular reductive elimination of H_2 (a process not accessible for the more hindered TMP or TTiPP complexes).[66] Then, thermal homolytic bond splitting of the Rh–Rh bond allows formation of a reactive mononuclear Rh^{II}(alkene) adduct, which subsequently reacts with H_2 or $[Rh^{III}(por)(H)]$ to abstract a hydrogen atom to give the "insertion" product $[Rh^{III}(por)(CH_2CH_2R)]$. Similar "insertions" of alkenes into the Rh–H bond of $[Rh^{III}(TPP)(H)]$ (via similar radical pathways) have been used to obtain $Rh^{III}–CH_2–$(alkyl)–Nu*H* species (Nu*H* = OH, NH) using alkenes functionalized with end-on -OH and -NH functionalities. Under basic conditions, intramolecular S_N2-type attack of the Nu at the α-carbon atom of $Rh^{III}–CH_2–$(alkyl)–Nu yields $[Rh^{I}(TPP)]^{-}$ and cyclic organic products [–CH_2–(alkyl)–Nu–], see Figure 19. Protonation of $[Rh^{I}(TPP)]^{-}$ then allows regeneration of $[Rh^{III}(TPP)(H)]$. The combination of these reactions constitutes a new method for selective intramolecular anti-Markovnikov hydrofunctionalization of alkenes with O–H and N–H functionalities.[67] In this way three- and five-membered ring compounds (epoxides, furan deriv-

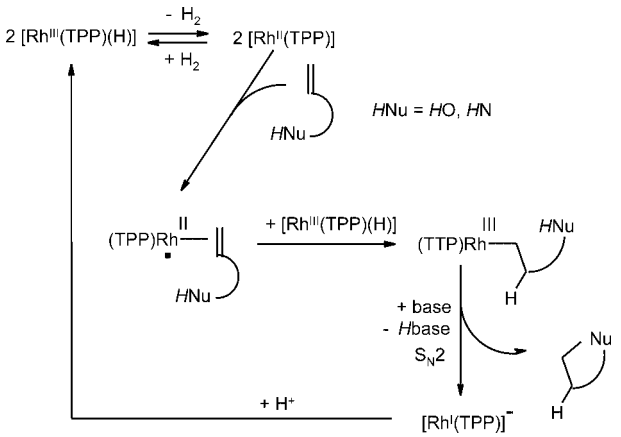

Figure 19. Selective intramolecular anti-Markovnikov hydrofunctionalization of alkenes with O–H and N–H functionalities via radical insertion of alkenes in the Rh–H bond.

 © 2007 Wiley-VCH Verlag GmbH & Co. KGaA, Weinheim

atives, pyrrolidine derivatives) were readily obtained. Formation of four- or six-membered rings proved not possible, and lead to regeneration of the starting alkenes instead (by a net β-hydrogen elimination).

The (TPP)Rh system efficiently mediates all steps, but the system is not capable of mediating the anti-Markovnikov hydro-functionalization reactions in a one-pot catalytic reaction. So far, the reaction conditions required for the different reaction steps proved incompatible.

3.2.3. [M^{II}(por)(alkene)] Intermediates in Reactions of [M^{III}(por)(alkyl)] Species with Nitroxyl Radicals

[M^{II}(por)(alkene)] species (M = Rh, Ir) also seem to be important intermediates in reactions of [M^{III}(por)(alkyl)] species with TEMPO and related nitroxyl radicals (M = Rh, Ir, por = TTP, TMP and some less common OMP, BTPP and BOCP porphyrinato ligands shown in Figure 20).

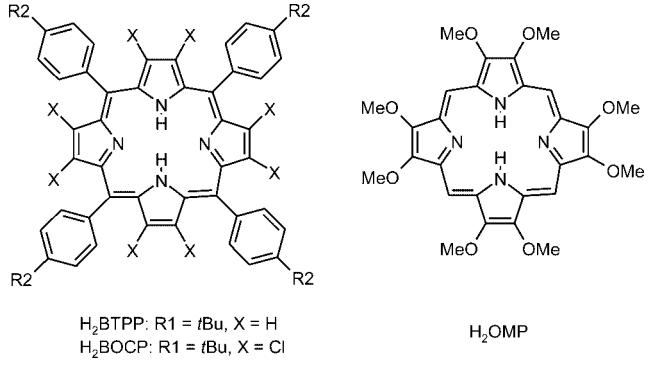

Figure 20. Ligand coding of the porphyrins BTPP, BOCP and OMP.

The [M^{III}(por)(alkyl)] complexes lacking β-hydrogen atoms do not react with nitroxyl radicals, but (por)Rh–alkyl species with β-hydrogen atoms eliminate alkene fragments upon heating in the presence of TEMPO.[68,69] For R = –CH$_2$–CH$_2$–Ph, formation of styrene was confirmed with NMR (Figure 21).

Abstraction of β-hydrogen atoms from alkyl species [M^{III}(por)(–CH$_2$CH$_2$R)] yields alkyl radical species [M^{III}(por)(–CH$_2$CHR$^{\cdot}$)], which are in fact the same activated β-alkyl radicals resulting from increasing the M–C–C angle of [M^{II}(por)(CH$_2$=CHR)] species. These [M^{III}(por)(–CH$_2$CHR$^{\cdot}$)] species should thus easily relax to the more stable alkene complexes [M^{II}(por)(CH$_2$=CHR)]. Because [Rh^{II}(por)] species have only a weak affinity for alkenes,[63] [M^{II}(por)(CH$_2$=CHR)] should readily lose the alkene (Figure 21). The resulting 15 VE [Rh^{II}(por)] species subsequently react with TEMPO to form [Rh^{III}(por)(CH$_3$)] by a C–C bond activation reaction with net abstraction of a methyl radical from TEMPO. Formation of [Rh^{II}(TMP)(R)] species by a net abstraction of an alkyl radical R$^{\cdot}$ from a nitroxyl radical (R′R$_2$C)$_2$NO$^{\cdot}$ has also been observed for isolated [Rh^{II}(TMP)] species in the presence of nitroxyl radicals (see Figure 21).[70] The mechanisms of the latter reactions are not very clear yet.

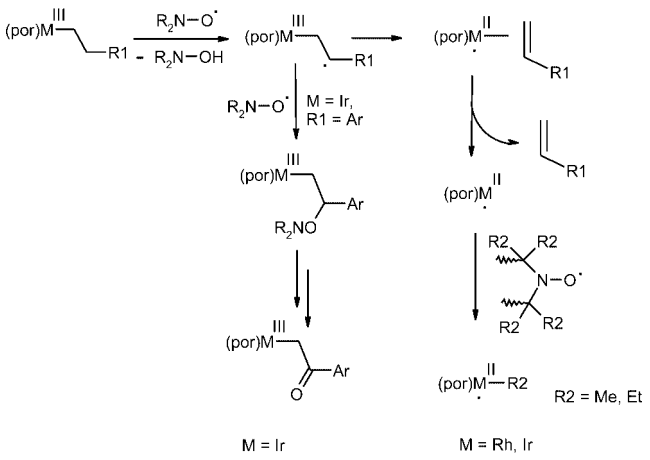

Figure 21. Reaction of TEMPO and related nitroxyl radicals with [M^{III}(por)(alkyl)] species (M = Rh, Ir) via [M^{II}(por)(alkene)] intermediates.

For the analogous iridium complexes [Ir^{III}(TTP)(R)], similar results were obtained upon reaction with TEMPO. Complexes lacking β-hydrogen atoms did not react, and non-aromatic alkyl complexes eliminate alkenes allowing formation of [Ir^{III}(TTP)(CH$_3$)] by C–C activation of TEMPO by [Ir^{II}(TTP)]. Arylethyl complexes [Ir^{III}(TTP)(–CH$_2$CH$_2$Ar)], however, reveal different products, which further support the proposed radical abstraction mechanism.[71] Under N$_2$, TEMPO oxidizes the [Ir^{III}(TTP)(–CH$_2$CH$_2$Ar)] species selectively at the β position to yield [Ir^{III}(TTP){–CH$_2$C(O)Ar}] (Figure 21). The mechanism proposed for this reaction involves abstraction of a β-hydrogen atom from [Ir^{III}(TTP)(–CH$_2$CH$_2$Ar)] by TEMPO to give [Ir^{III}(TTP)(–CH$_2$CH$^{\cdot}$Ar)] and TEMPO*H*. Apparently, due to stabilization of the β-carbon radical by the aromatic group and a substantially stronger Ir–C bond compared to a Rh–C bond, this species is sufficiently long-lived to react with a second TEMPO moiety. Coupling of the [Ir^{III}(TTP)(–CH$_2$CH$^{\cdot}$Ar)] radical with the TEMPO radical was proposed to yield a [Ir^{III}(TTP)(–CH$_2$CHAr–O–NR$_2$)] intermediate. The latter could then decompose to the observed [Ir^{III}(TTP){–CH$_2$C(O)Ar}] species, either directly through a hydrogen shift (with elimination of R$_2$NH) or by abstraction of the remaining β-hydrogen by an additional TEMPO moiety.

3.3 Reactivity of M^{II}(alkene)(N-ligand) Species Bearing Allylic Hydrogen Atoms

Reaction of [Rh^{II}(OEP)] with alkenes (CH$_2$=CHR) containing allylic hydrogen atoms such as allylbenzene (R = CH$_2$Ph), allyl cyanide (R = CH$_2$CN) and 1-hexene (R = CH$_2$C$_3$H$_8$) results in formation of σ-allyl complexes [Rh^{III}(OEP)(CH$_2$CH=CHR)] in about 50% yield (Figure 22).[58] A more detailed study concerning the behavior of [Rh^{II}(OEP)] towards propene was reported.[72] Propene initially forms the alkyl-bridged species [Rh^{III}(OEP){μ$_2$-CH$_2$CH(Me)-}Rh^{III}(OEP)]. This species reveals an interest-

 © 2007 Wiley-VCH Verlag GmbH & Co. KGaA, Weinheim

ing 1,2-exchange of the two metal sites, reflecting the lability of the Rh–C bond. The species is not stable and converts over the course of some days to a 1:1 mixture of the σ-allyl species [Rh^{III}(OEP)($CH_2CH{=}CH_2$)] and the propyl species [Rh^{III}(OEP)($CH_2CH_2CH_2$)], which likely involves a net transfer of an allylic hydrogen atom from [Rh^{II}(OEP)-(propene)] to another [Rh^{II}(OEP)(propene)] species (obtained from [Rh^{III}(OEP)(μ_2-CH_2CH(Me)-)Rh^{III}(OEP)] by Rh–C homolysis), see Figure 22.

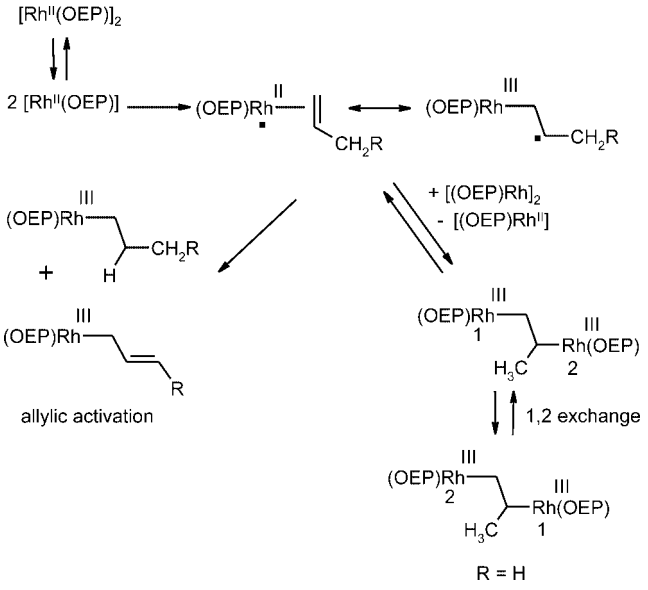

Figure 22. Reactivity of [Rh^{II}(por)] species towards alkenes containing allylic hydrogen atoms.

A comparable allylic activation of methyl methacrylate [CH_2=C(Me)(COOMe)] was reported to give a 1:1 mixture of [Rh^{III}(OEP){CH_2C(COOMe)=CH_2}] and [Rh^{III}(OEP)-{CH_2CH(Me)(COOMe)}]. Reaction of the sterically more hindered [Rh^{II}(TMP)] with methyl metacrylate yields a 1:1 mixture of [Rh^{III}(TMP){CH_2C(COOMe)=CH_2}] and [Rh^{III}(TMP)(H)]. The reactions were proposed to proceed by abstraction of an allylic hydrogen atom from the metallo-radical alkene complex [Rh^{II}(por){CH_2=C-(Me)(COOMe)}] by the metallo-radical [Rh^{II}(por)] to yield directly the σ-allyl complex [Rh^{III}(por){CH_2C-(COOMe)=CH_2}] and the hydride species [Rh^{III}(por)(H)]. As described above, the OEP complexes allow "insertion" reactions into the Rh–H bond, which for methyl methacrylate yields [Rh^{III}(OEP){CH_2CH(Me)(COOMe)}]. Alkene "insertion" into the Rh–H bond of the TMP complexes does not occur, presumably for steric reasons.

Further evidence for allylic C–H activation of M^{II}(α-alkene) species proceeding via bimolecular abstraction of an allylic hydrogen by another M^{II} species was gathered by studying the decomposition of dicationic [M^{II}(cod)(N_3-ligand)]$^{2+}$ species. Although the [M^{II}(cod)(N_3-ligand)]$^{2+}$ species can be isolated as pure compounds, in solution they decompose through an allylic C–H activation process. The [M^{II}(N_3-ligand)(cod)]$^{2+}$ complexes invariably decompose to 1:1 mixtures of [M^{III}(N_3-ligand)(cyclooctadienyl)]$^{2+}$ and species that could be described as "protonated M^{I}(cod)" species. For the "protonated M^{I}(cod)" species the position of the proton depends on the nature of the metal. The proton ends-up at the metal for iridium, forming [Ir^{III}(H)(N_3-ligand)(cod)]$^{2+}$, and at the N_3-ligand Py moiety for rhodium, forming [Rh^{I}(N_3-ligand*H*)(cod)]$^{2+}$ (Figure 23).[41,42] The reaction rates decrease upon increasing the steric bulk of the N_3-ligand.

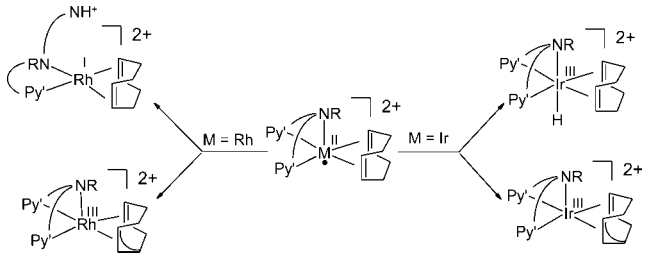

Figure 23. Selective conversion of the [M^{II}(N_3-ligand)(cod)]$^{2+}$ complexes to allyl species [M^{III}(cyclooctadienyl)(N_3-ligand)]$^{2+}$ (M = Rh, Ir) and equimolar amounts of [Rh^{I}(N_3-ligandH)(cod)]$^{2+}$ (for M = Rh) or [Ir^{III}(H)(N_3-ligand)(cod)]$^{2+}$ (for M = Ir).

The product ratio can be explained by a hydrogen-atom transfer from one M^{II}(cod) species to another M^{II}(cod) species. An electron-transfer (ET) disproportionation reaction between two M^{II}(cod) species to give M^{I}(cod) and M^{III}-(cod) followed by a proton transfer from an allylic position of M^{III}(cod) to M^{I}(cod) was ruled out.[41,42] A direct hydrogen-atom abstraction (at least in case of the more hindered Bn-dla ligands) of an allylic hydrogen atom of M^{II}(cod) by another M^{II} species also seems unlikely, because the metal is rather shielded by the N_3-ligand PyMe bulk. The kinetic rate expression $v = k_{obsd.}$ [M^{II}]^2 in acetone, with $k_{obsd.} = k$[H^+][S] and [S] being the concentration of additional coordinating reagents (MeCN), is in agreement with a solvent-assisted dissociation of one of the pyridine donors.[42] Pyridine dissociation results in formation of more open, reactive species. Protonation of the non-coordinating pyridine increases the concentration of this species, and thus [H^+] appears in the kinetic rate expression. Both the rate expression and the kinetic activation parameters ($\Delta H^{\#}$ = 50 ± 8 kJ mol^{-1}, $\Delta S^{\#}$ = –113 ± 42 J K^{-1} mol^{-1} and $\Delta G_{289K}{}^{\#}$ = 84 ± 21 kJ mol^{-1}) are in agreement with a subsequent bimolecular hydrogen-atom transfer from an allylic M^{II}(cod) position to another M^{II} species (Figure 24).

Formation of M^{III}(allyl) species from M^{II}(alkene) species (M = Rh, Ir) bearing allylic hydrogen atoms seems to be a more general decomposition pathway of such species. As described above, it has been observed as a decomposition pathway of [M^{II}(cod)(N_3-ligand)]$^{2+}$ compounds, and in reactions of α-alkenes with [Rh^{II}(por)] species. Formation of [Rh^{III}(R_3-Cp)(allyl)]$^+$ (allyl) species was also reported for in situ generated [Rh^{II}(R_3-Cp)(cod)]$^+$.[73] Furthermore, one-electron oxidation of [Ir^{I}(Me_2tpa)(propene)]$^+$ with [Ag]PF_6 in acetonitrile afforded the Ir^{III}(allyl) species [Ir^{III}(η^3-propenyl)(Me_2tpa)]$^{2+}$ in about 50% yield (Me_2-tpa = *N*-(2-pyridylmethyl)-*N*,*N*-bis[(6-methyl-2-pyridyl)methyl]amine), see Figure 25.[42]

 © 2007 Wiley-VCH Verlag GmbH & Co. KGaA, Weinheim

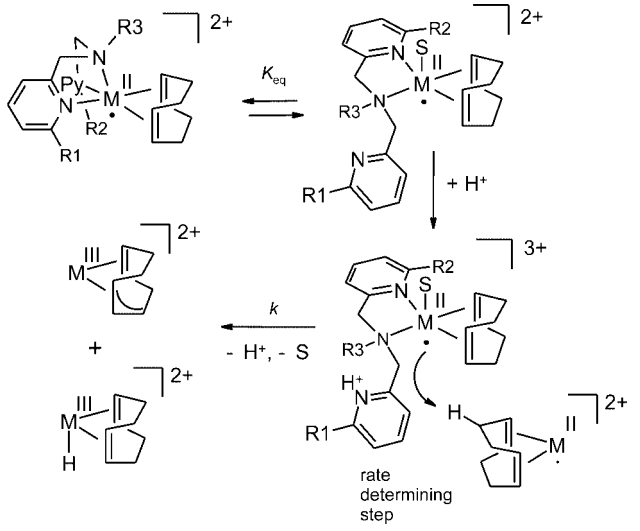

Figure 24. Proposed mechanism for the hydrogen-atom transfer between two M^{II}(cod) species.

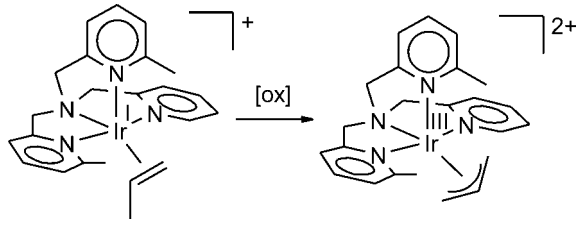

Figure 25. Formation of an Ir^{III}(allyl) species by oxidation of $[Ir^{I}(propene)(Me_2tpa)]^+$.

Notable exceptions to the general tendency of M^{II}(α-alkene) species (M = Rh, Ir) decomposing to M^{III}(allyl) species are the complexes $[M^{II}(C_6Cl_5)_2(1,5\text{-cod})]$ (M = Rh, Ir), $[Rh^{II}(\eta^5\text{-}C_5Ph_5)(1,5\text{-cod})]^+$ and $[Rh^{II}(\eta^5\text{-}C_5Ph_5)(1,3\text{-cod})]^+$, which are stable at room temp.[33–35] These species are sterically rather shielded around the metal, which might explain their relative stability. This can be taken as a further indication that such decomposition pathways proceed through bimolecular allylic H-atom abstraction by metal-centered radicals.

4. M^{II}(alkene) Species as Intermediates in Rh- and Ir-Catalyzed Alkene Oxygenation?

Though less well-known than Pd, both Rh and Ir are able to catalyze oxidation of alkenes with O_2 and H_2O_2,[74] Rh generally being more effective than Ir. Oxidation of terminal alkenes almost invariably results in formation of methyl ketones. Oxidation of internal alkenes leads to epoxides, allylic alcohols, ethers or ketones. The mechanistic picture of rhodium-catalyzed oxidations is complex with several mechanisms being proposed for various catalysts under different conditions: Wacker-type reactivity, reaction of a metal peroxide with the alkene to a peroxymetallacycle, formation of an intermediate hydroperoxo or alkylperoxo complex which reacts with the alkene, and some early work on alkene oxidation with peroxo Rh and Ir complexes was shown to proceed through free-radical pathways. In attempts to collect mechanistic information about rhodium- and iridium-catalyzed oxygenation of alkenes, stoichiometric oxygenation of N-ligand Rh^{I}- and Ir^{I}-alkene complexes by O_2 has been investigated in detail over the past years.[74,75] Oxygenation products strongly vary with the N-ligand, the alkene (ethene, propene, 1,5-cyclooctadiene and other dienes) and the central metal (Rh, Ir), see Figure 26.

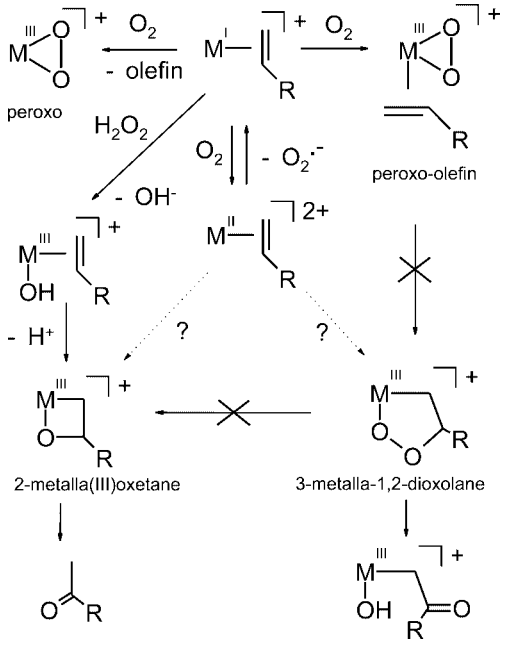

Figure 26. Oxygenation products from reaction of $[M^{I}(alkene)(N\text{-ligand})]^+$ species with O_2.

The reactivity of N-ligand Rh^{I} and Ir^{I}-alkene fragments towards dioxygen varies between alkene displacement, formation of mixed O_2-alkene complexes, C–O bond formation (giving a 3-metalla-1,2-dioxolane), and combined O–O bond breaking/C–O bond making (giving a 2-metallaoxetane). Isolated peroxo complexes showed no further reactivity towards alkenes or alkene complexes, and isolated peroxo–ethene complexes did not contract to the corresponding peroxo-metallacycles (Figure 26). Isolated 3-metalla-1,2-dioxolanes, which were proposed as key-intermediates in the catalytic reactions, do not eliminate methyl ketones at all, but instead convert to formylmethyl-hydroxido complexes (Figure 26). The isolated 2-metalla(III)oxetanes, despite not being proposed in the catalytic reactions previously, proved actually much more likely candidates to be such key-intermediates. These species readily eliminate methyl ketones (acetaldehyde in case of the ethene precursor); the exact same products as obtained in the catalytic reactions. Formation of methyl ketones could not be demonstrated for any of the peroxo, peroxo–alkene or metal-dioxolane species. An important unanswered question is the mechanism of 2-metalla(III)oxetane formation in these reactions. Formation of 2-metalla(III)oxetanes from M^{I}-(alkene) and H_2O_2 seems straightforward (a net OH^+ transfer to the metal, followed by alkene insertion into the M^{III}–OH fragment,[74] see Figure 26), but the essential C–O

 © 2007 Wiley-VCH Verlag GmbH & Co. KGaA, Weinheim

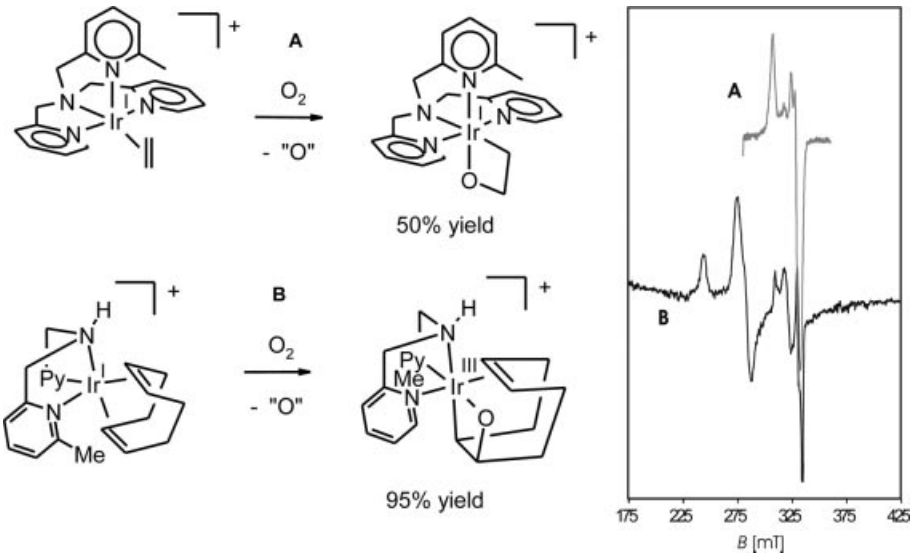

Figure 27. Formation of metallaoxetanes from reaction of Ir^{I}-alkene fragments with O_2 and the detection of possible Ir^{II} and $Ir–O_2^{\cdot-}$ intermediates.

bond making step in oxygenation reactions of M^{I}(alkene) species with O_2 remains rather unclear.

Notably, for some of the more interesting reactions in Figure 26 leading to C–O bond formation with O_2, paramagnetic species were detected accompanying product formation. For example, reaction of $[Ir^{I}$(ethene)(Metpa)$]^+$ and $[Ir^{I}$(cod)(bpaMe)$]^+$ with O_2 in CH_2Cl_2 leads to formation of the corresponding 2-metallaoxetanes (Figure 27) in about 50% and 95% yield, respectively. These reactions consume only one O atom of O_2 per metal complex. The fate of the other O atom is not known.[76,77] Interestingly, during the course of these reactions, weak EPR signals were observed pointing to formation of paramagnetic Ir species, which are either intermediates or side products.[78,79]

To shed some light on the possible role of paramagnetic M^{II}(alkene) complexes in the essential C–O bond formation steps of these reactions, the reactivity of isolated $[M^{II}$-(alkene)(N-ligand)$]^{2+}$ species towards O_2 has been investigated in detail.

Treatment of $[Ir^{II}(Me_3tpa)(ethene)]^{2+}$ and $[M^{II}$(dpa)-(cod)$]^{2+}$ with dioxygen leads to formation of new EPR spectra.[8,38,41,42] A substantial decrease in the *g* anisotropy indicates a shift of the spin density from the metal to dioxygen. The observed spectra are consistent with formation of the superoxide complexes $[Ir^{III}(O_2^{\cdot})(Me_3tpa)(ethene)]^{2+}$ and $[M^{III}(O_2^{\cdot})$(dpa)(cod)$]^{2+}$. Formation of superoxide complexes from $[M^{II}(N_3$-ligand)(cod)$]^{2+}$ and O_2 appears to be reversible. Increasing the N-ligand steric bulk decreases the oxygen affinities. Reaction of $[Rh^{II}$(pla)(cod)$]^{2+}$ with O_2 only leads to small concentrations of $[Ir^{III}(O_2^{\cdot})$(pla)(cod)$]^{2+}$. The $[Rh^{II}$(R-bla)(cod)$]^{2+}$ (R = H, Bn) and $[Rh^{II}$(pla)-(nbd)$]^{2+}$ complexes proved to be air stable as a result of shielding by the bulky Py–Me groups.

No C–O bond-formation reactions were observed for any of the $[M^{III}(O_2^{\cdot})(N_3$-ligand)(cod)$]^{2+}$ complexes. These species decompose to the same mixture of compounds as observed for $[M^{II}(N_3$-ligand)(cod)$]^{2+}$ in absence of O_2 (see above).[41,42] Thus, unless these species play a role as co-catalysts, it seems unlikely that M^{II}(cod) species are intermediates in formation of 2-metalla-oxetanes from M^{I}(cod) complexes and O_2. For ethene complexes the situation might be different. $[Ir^{II}(Me_2tpa)(ethene)]^{2+}$ reacts rapidly with O_2, but not selectively (all solvents). The fate of the more hindered analog $[Ir^{III}(O_2^{\cdot})(Me_3tpa)(ethene)]^{2+}$ depends on the solvent. The reaction in acetone leads to yet unidentified products. The reaction in MeCN takes a different course (as described hereafter). To shed some light on these reactions, $[Ir^{III}(O_2^{\cdot})$(ethene) $(Me_3tpa)]^{2+}$ was trapped with DMPO.[8] This led to dissociation of ethene and formation of a C–O bond between the superoxide and DMPO (Figure 28). The peroxide-bridged species likely rearranges to a species with an acetal group, thus explaining the absence of proton hyperfine couplings in EPR. The unusual large N hyperfine coupling ($A^{N}_{average}$ = 74 MHz) compared to trapped organic radicals (A^{N} = 42 MHz) indicates that the unpaired electron resides mainly at the nitrogen part of the nitroxyl group.[80] Therefore, DMPO appears to be coordinated to the iridium center. This is confirmed by the unusually large *g* anisotropy (g_{11} = 2.036, g_{22} = 2.014, g_{33} = 1.986) for a DMPO-trapped radical (Figure 28). At room temperature this species converts to a diamagnetic species with a coordinated oxygenated DMPO fragment. This likely involves hydrogen abstraction from the solvent and elimination of H_2O (Figure 28). Remarkably, such obtained solvent radicals were trapped by Ir^{II} species, rather than the spin-trap DMPO. ESI-MS indicated clear formation of $[Ir^{III}(CH_2CN)(Me_3tpa)]^{2+}$ in acetonitrile and $[Ir^{III}(CH_2COCH_3)(Me_3tpa)]^{2+}$ in acetone.

The reactions of $[Ir^{III}$(ethene)$(N_4$-ligand)$]^{2+}$ species with dioxygen in the presence of MeCN result in formation of $Ir^{III}–CH_2C(O)H$ species. These reactions likely proceed via $[Ir^{III}(CH_2CH_2^{\cdot})(N_4$-ligand)(MeCN)$]^{2+}$ intermediates, which are easily formed upon contact with MeCN as described in section 3.1.1 (Figure 10). Quite likely, the triplet biradical

 © 2007 Wiley-VCH Verlag GmbH & Co. KGaA, Weinheim

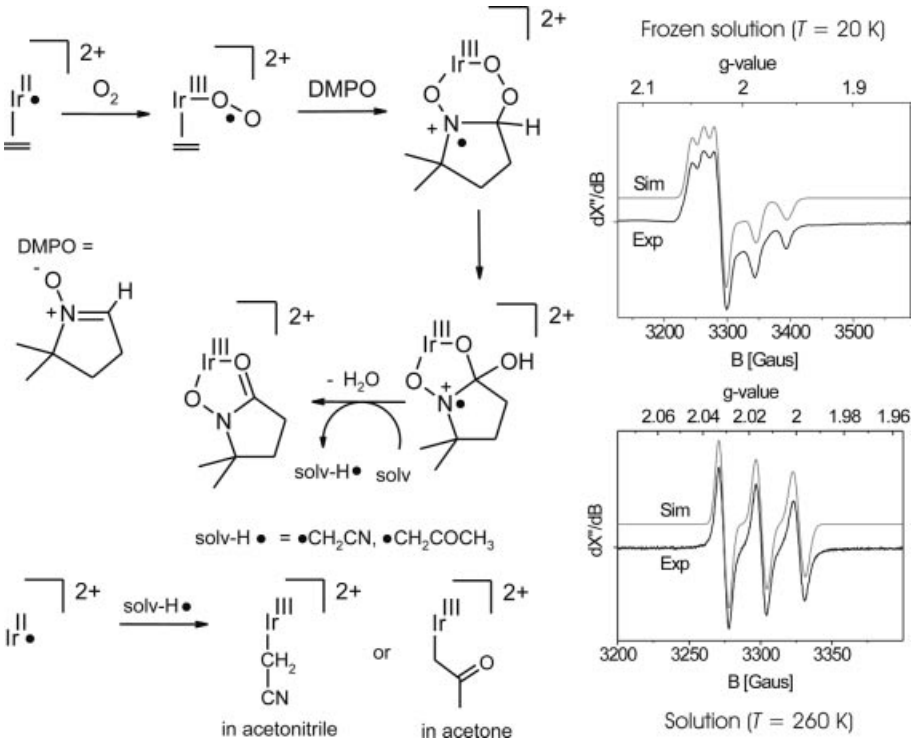

Figure 28. Proposed mechanism for the oxygenation of DMPO at Ir^{II} and the EPR spectra belonging to the paramagnetic Ir–O_2–DMPO intermediate.

dioxygen reacts directly with the β-carbon-centered radical of $[Ir^{III}(CH_2CH_2^{\cdot})(N_4\text{-ligand})(MeCN)]^{2+}$ to give Ir^{III}–$CH_2CH_2OO^{\cdot}$ species. The latter alkylperoxo radical species then abstracts a hydrogen atom from acetonitrile, leading to a hydroperoxo intermediate Ir^{III}–CH_2CH_2OOH, which eliminates water to give the observed Ir^{III}–$CH_2C(O)H$ species (Figure 29).[8,38] Also in this case, the remaining solvent radical is trapped by the Ir^{II} starting material. An alternative mechanism via $[Ir^{III}(O_2^{\cdot})(N_4\text{-ligand})(ethene)]^{2+}$ species cannot be ruled out completely though.

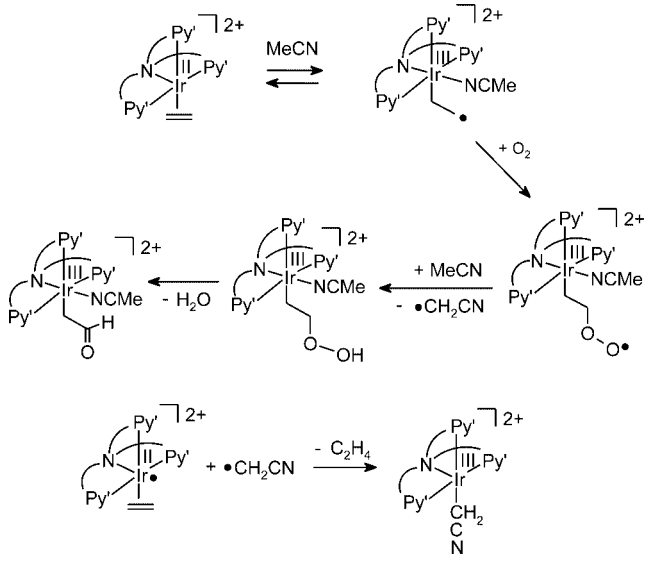

Figure 29. Proposed mechanism for the mono-oxygenation of $[Ir^{II}(Me_3tpa)(ethene)]^{2+}$ in acetonitrile.

With the exception of M^{II}(ethene) species, M^{II}(α-alkene) species are not very likely to be directly involved in the C–O bond-making processes of rhodium- and iridium-catalyzed alkene oxygenation reactions described by Mimoun, Read, Drago and others.[74] It seems that even in the presence of O_2, allylic C–H activation is the preferred kinetic decomposition pathway of such α-alkene complexes. Generally, such obtained (kinetically inert) M^{III}(allyl) species are not reactive towards O_2. M^{II} species without a coordinated alkene might be involved though, perhaps facilitating formation of peroxides from O_2 and a sacrificial reductant (often an alcohol in the catalytic reactions). Such peroxides easily react with M^{I}(α-alkene) species to yield methyl ketones [via 2-metalla(III)oxetanes as intermediates, as described above, see Figure 26].

Somewhat related to this topic, M^{II}(nbd) species are potential Wacker-type catalysts for oxidation of norbornadiene to norbornenone. Dicationic $[M^{II}(bis\text{-alkene})(N_3\text{-ligand})]^{2+}$ species are stable towards ET disproportionation. The situation, however, changes in the presence of chloride anions, which trigger ET disproportionation. Formation of dicationic $[M^{III}(Cl)]$ products is probably less unfavorable than formation of tricationic M^{III} species. Interestingly, Cl^- triggered disproportionation of $[Rh^{II}(pla)(nbd)]^{2+}$ in the presence of water or alcohols led to formation of $[Rh^{I}(pla)(nbd)]^{+}$ and $[\{Rh^{III}(Cl)(nbd\text{-}OR)(pla)\}_2]^{2+}$ (Figure 30). The latter species likely result from a Wacker-type attack of water/alcohols to the $[Rh^{III}(Cl)(pla)(nbd)]^{2+}$ intermediate.

 © 2007 Wiley-VCH Verlag GmbH & Co. KGaA, Weinheim

Heating $[\{Rh^{III}(Cl)(nbd\text{-}OH)(pla)\}_2]^{2+}$ in the presence of an excess of the oxidant $FeCl_3$ led to catalytic formation of norbornenone, albeit with only low total turnover numbers.[40] These reactions are nevertheless noteworthy, because no Wacker oxidation catalysts for norbornadiene have been reported and oxidation of other bis-alkenes also gives poor results or diketones.[81] The main problem with palladium-mediated Wacker oxidation of bis-alkenes is that attack of OH^- or H_2O to the Pd^{II}(bis-alkene) complex usually yields a η^3-3-hydroxy-enyl σ–π complex, in which coordination of the second double bond prevents easy β elimination.[82]

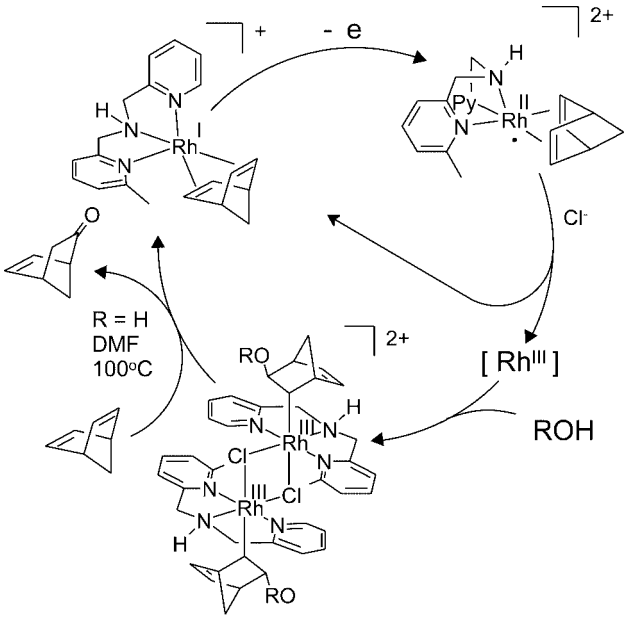

Figure 30. Catalytic formation of norbornenone through chloride-triggered disproportionation of $[Rh^{II}(pla)(nbd)]^{2+}$.

5. Rh^{II}-Alkene Species as Intermediates in Catalytic Carbene Transfer Reactions?

Diamagnetic dinuclear carboxylate-bridged Rh^{II}–Rh^{II} species have been extensively studied as a catalysts for carbene-transfer reactions.[83] It has always been assumed that the Rh^{II}–Rh^{II} species stay intact during catalysis, but this was never really proven. A study by Bergman clearly reveals that mononuclear Rh^{II} species can also be active catalysts for carbene-transfer reactions. $[Rh^{II}(Cl)(Tf)(bisoxozaline)]$ (Tf^- = triflate) is an active alkene cyclopropanation catalyst. Although the catalytic precursor does not contain Rh-alkene fragment, the carbene-transfer reaction is highly likely to involve such species as intermediates.

The catalytic activity is enhanced by addition of $NaBAr_F$, yielding $[Rh^{II}(bisoxozaline)(Cl)(CH_2Cl_2)]^+$ {BAr_F^- = tetrakis[3,5-bis(trifluoromethyl)phenyl]borate}.[84] The active species is believed to be a low-valent 15 VE species with two (bis)oxozaline nitrogen atoms in mutual *trans* positions and a chlorido ligand occupying a third position. Two sites of the rhodium center are sterically hindered by the (bis)-oxozaline methyl groups and the bridging arene. In the *trans* position to the chloro ligand, a labile triflate anion or dichloromethane ligand is bound allowing easy formation of a vacant site. In the presence of diazoacetates, dimerization to fumarates and maleates takes place, indicative of carbene-transfer reactions.[84] Also selective cyclopropanation (Figure 31) of alkenes and formation of aziridines from imines is catalyzed by these complexes. With these results, one might consider open-shell species to play an active role in other carbene-transfer reactions as well.

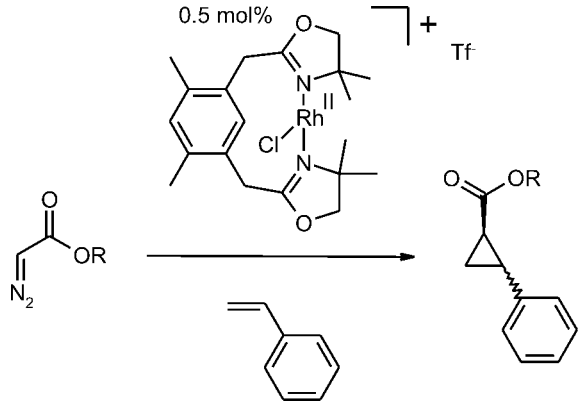

Figure 31. Cyclopropanation of styrene-mediated by a mononuclear $[Rh^{II}(Cl)_2(benbox)]^+$ complex.

For example, in the recently discovered Rh-mediated stereoselective polymerization of carbenes from diazoacetates, Rh^{II}(alkene) radicals might well be important (Figure 32).[85] It was shown that $[Rh^{I}$(prolinate)(cod)] is a catalyst precursor for polymerization of carbenes from diazoacetates, leading to formation of new, stereoregular (most likely syndiotactic) ester-functionalized polymethylenes. This new family of polymers contain a functional side group at each carbon of the polymer backbone. Polymers with molecular weights up to 190000 (M_w) were obtained as solid materials with interesting material properties. Notably, only about 1% of the Rh material becomes active in the polymerization reaction. Therefore, it is interesting to note that EPR measurements have indicated formation of (very) low concentrations of radical species during the reaction.[78] Whereas these radicals are just side products, or are involved as intermediates in the polymerization reaction needs to be established in future studies.

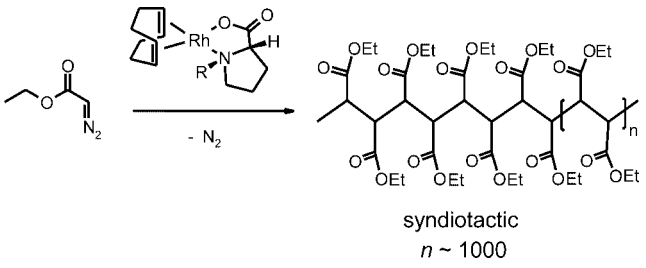

Figure 32. Are radical species involved in the recently discovered stereoselective Rh-mediated polymerization of "carbenes"?

 © 2007 Wiley-VCH Verlag GmbH & Co. KGaA, Weinheim

6. Conclusions

Paramagnetic rhodium and iridium alkene species, especially the nitrogen-ligand-based $[M^{II}(por)(alkene)]$ and $[M^{II}(alkene)(N\text{-ligand})]^{2+}$ species, reveal a remarkable variety of radical-type reactions. The five-coordinate $[M^{II}(por)(alkene)]$ species, for which mixing of the d_{z^2} and alkene orbitals ensures that part of the unpaired electron density is located at the olefinic ligand, are especially reactive. These alkene adducts cannot be isolated due to fast M–C and C–C radical couplings leading to alkylene-bridged species. Attempts to sterically prevent these reactions leads to alkene adducts which easily lose the alkene. Alkenes bind stronger to dicationic five-coordinate $[M^{II}(N_4\text{-ligand})]$ and $[M^{II}(N_3\text{-ligand})]$ complexes containing neutral tetradentate or tridentate podal $N\{CH_2Py\}_n$ (n = 2,3) type ligands. The orbital arrangement of these species is different, so that the d_{z^2} orbital containing the unpaired electron interacts with a N_{amine} donor instead of the alkene. Consequently, the alkene fragments do not reveal much radical-type reactivity without activation. The situation changes upon binding of a strong coordinating solvent (e.g. MeCN), resulting in a donor-induced shift of the spin-density from the metal to the π* orbitals of the alkene. Most of the spin density of the resulting $M^{III}(NCMe)(CH_2CH_2^{\cdot})$ species is located at the β-carbon of the "slipped" alkene, thus triggering radical-type reactivity at the alkene/ethyl radical fragment. This donor-induced shift of the spin density from the metal to the alkene constitutes a new approach to tuning the reactivity of open-shell metal-alkene species.

Stable examples of M^{II}(α-alkene) complexes, containing reactive allylic hydrogen atoms, all have their metal center sterically protected. All other examples tend to decompose with formation of M^{III}(allyl) and M^{III}(H) species. The presence of unpaired spin density at the alkene is of less concern for these decomposition pathways, as they proceed through a dinuclear pathway in which an allylic hydrogen atom of one M^{II}(alkene) species is abstracted by another M^{II}(alkene) radical *at the metal*.

Although limited in number, there are a few examples in which experimental evidence for the involvement of paramagnetic rhodium and iridium species in catalytic reactions is quite strong. For example, paramagnetic intermediates might play a role in the catalytic alkene oxygenation reactions described in the 1970s and early 1980s by Mimoun, Drago, Read and others.[74,75] Whether or not this concerns paramagnetic alkene species remains a question. M^{II}(α-alkene) species perhaps too easily undergo allylic C–H activation, making them less attractive candidates to be intermediates in the C–O bond formation processes. C–O bond formation through oxidation of diamagnetic M^{I}(alkene) species (by peroxides for example) to 2-metalla(III)oxetane intermediates seems a more likely pathway. Paramagnetic M^{II} species might nevertheless be important in these reactions, e.g. by facilitating peroxide formation from O_2 and a sacrificial reductant (e.g. an alcohol). On the other hand, the situation may strongly depend on the olefinic substrate. Model reactions of $[Ir^{II}(ethene)(N_4\text{-ligand})]^{2+}$ species with O_2 have revealed that with these ethene species, lacking reactive allylic hydrogens, facile C–O bond formation is certainly possible. This reaction likely proceeds via external attack of the "alkene radical" species $M^{III}(NCMe)(CH_2CH_2^{\cdot})$ by O_2. This demonstrates the potential of donor induced generation of "alkene radicals" from M^{II}(alkene) species as a new approach to steer the reactivity of open-shell M(alkene) species.

Catalytic cyclopropanation of alkenes with ethyl diazoacetate mediated by well defined Rh^{II}(alkene) species has been demonstrated,[84] and it is well possible that open-shell M^{II}(alkene) species are also active in other carbene-transfer reactions. Wacker-type oxidation of norbornadiene to norbornenone is another reaction which definitely proceeds via discrete Rh^{II}(alkene) species.[40]

The rich chemistry displayed by paramagnetic M(alkene) species is fascinating. Whether or nor these species will turn out to be important in new or existing catalytic reactions remains a question to be answered in the future.

Acknowledgments

This work was supported by the Netherlands Organization for Scientific Research (NWO-CW), the Radboud University Nijmegen and the University of Amsterdam.

[1] a) D. Astruc, Electron-Transfer and Radical Processes, in: *Transition-Metal Chemistry*, VCH, New York, **1995**; b) M. C. Baird, *Chem. Rev.* **1988**, *88*, 1217–1227; c) W. C. Trogler (Ed.), Organometallic Radical Processes, *Journal of Organometallic Chemistry Library*, vol. 22, Elsevier, Amsterdam, **1990**; d) N. G. Connelly, *Chem. Soc. Rev.* **1989**, *18*, 153–185; e) M. Channon, M. Julliard, J. C. Poite (Eds.), Paramagnetic Organometallic Species, in: *Activation/Selectivity, Catalysis*, NATO ASI series, Kluwer Academic, Dordrecht, **1987**; f) L. A. MacAdams, G. P. Buffone, C. D. Incarvito, J. A. Golen, A. L. Rheingold, K. H. Theopold, *Chem. Commun.* **2003**, *10*, 1164–1165; g) C. Pariya, K. H. Theopold, *Curr. Sci.* **2000**, *78*, 1345–1351; h) J. D. Jewson, L. M. Liable-Sands, G. P. A. Yap, A. L. Rheingold, K. H. Theopold, *Organometallics* **1999**, *18*, 300–305; i) R. Poli, *Chem. Rev.* **1996**, *96*, 2135–2204; j) C. Limberg, *Angew. Chem. Int. Ed.* **2003**, *42*, 5932–5954; *Angew. Chem.* **2003**, *115*, 6112–6136.

[2] Rh^{II}(alkene) intermediates were considered as possible intermediates the catalytic isomerization of 1-nonene to 2-nonene, hydrogenation of ketones and alkenes and iridium-catalyzed carbonylation of alcohols to carboxylic acids has been claimed to involve Ir^{II} species; a) G. Strukul, M. Bonivento, M. Graziani, E. Cerna, N. Palladino, *Inorg. Chim. Acta* **1975**, *12*, 15–21; b) L. D. Tyutchenkova, V. G. Vinogradova, Z. K. Maizus, *Izv. Akad. Nauk SSSR, Ser. Khim.* **1978**, *4*, 773–777; c) S. Padhye, R. Yerande, R. P. Patil, A. A. Kelkar, R. V. Chaudhari, *Inorg. Chim. Acta* **1989**, *156*, 23–25.

[3] K. E. Toracca, L. McElwee-White, *Coord. Chem. Rev.* **2000**, *206–207*, 469–491.

[4] a) B. B. Wayland, S. Ba, A. E. Sherry, *J. Am. Chem. Soc.* **1991**, *113*, 5305–5311; b) A. E. Sherry, B. B. Wayland, *J. Am. Chem. Soc.* **1990**, *112*, 1259–1261; c) B. B. Wayland, S. Ba, A. E. Sherry, *Inorg. Chem.* **1992**, *31*, 148–150; d) X.-X. Zhang, B. B. Wayland, *Inorg. Chem.* **2000**, *39*, 5318–5325; e) X. X. Zhang, B. B. Wayland, *J. Am. Chem. Soc.* **1994**, *116*, 7897–7898; f) W. H. Cui, X. P. Zhang, B. B. Wayland, *J. Am. Chem. Soc.* **2003**, *125*, 4994–4995; g) W. H. Cui, B. B. Wayland, *J. Am. Chem. Soc.* **2004**, *126*, 8266–8274.

 © 2007 Wiley-VCH Verlag GmbH & Co. KGaA, Weinheim

[5] a) K. K. Pandey, *Coord. Chem. Rev.* **1991**, *121*, 1–42; b) D. G. DeWitt, *Coord. Chem. Rev.* **1996**, *147*, 209–246; c) D. G.H Hetterscheid, A. J. J. Koekkoek, H. Grüzmacher, B. de Bruin, *Progress in Inorganic Chemistry*, accepted.

[6] C. K. Jørgensen, *Oxidation numbers and oxidation states*, Springer, Berlin, Germany, **1969**.

[7] D. G. H. Hetterscheid, J. Kaiser, E. Reijerse, T. P. J. Peters, S. Thewissen, A. N. J. Blok, J. M. M. Smits, R. de Gelder, B. de Bruin, *J. Am. Chem. Soc.* **2005**, *127*, 1895–1905.

[8] D. G. H. Hetterscheid, M. Bens, B. de Bruin, *Dalton Trans.* **2005**, 979–984.

[9] N. G. Connelly, A. C. Loyns, M. A. Ciriano, M. J. Fernandez, L. A. Oro, B. E. Villarroya, *J. Chem. Soc., Dalton Trans.* **1989**, 689–691.

[10] B. E. Villarroya, L. A. Oro, F. J. Lahoz, A. J. Edwards, M. A. Ciriano, P. J. Alonso, A. Tiripicchio, M. T. Camellini, *Inorg. Chim. Acta* **1996**, *250*, 241–264.

[11] M. A. Casado, J. J. Pérez-Torrente, J. A. López, M. A. Ciriano, P. J. Alonso, F. J. Lahoz, L. A. Oro, *Inorg. Chem.* **2001**, *40*, 4785–4792.

[12] D. C. Boyd, N. G. Connelly, G. G. Herbosa, M. G. Hill, K. R. Mann, C. Mealli, A. G. Orpen, K. E. Richardson, P. H. Rieger, *Inorg. Chem.* **1994**, *33*, 960–971 and references cited therein.

[13] N. Kanematsu, M. Ebihara, T. Kawamura, *Inorg. Chim. Acta* **2001**, *323*, 96–104.

[14] J. M. Poblet, M. Bernard, *Inorg. Chem.* **1988**, *27*, 2935–2941.

[15] K. M. Kadish, T. D. Phan, L. Giribabu, E. Van Caemelbecke, J. L. Bear, *Inorg. Chem.* **2003**, *42*, 8663–8673.

[16] N. G. Connelly, O. D. Hayward, P. Klangsinsirikul, A. G. Orpen, P. H. Rieger, *Chem. Commun.* **2000**, 963–964.

[17] C. J. Adams, R. A. Baber, N. G. Connelly, P. Harding, O. D. Hayward, M. Kandiah, A. G. Orpen, *Dalton Trans.* **2006**, 1749–1757.

[18] a) C. G. Pierpont, C. W. Lange, *Prog. Inorg. Chem.* **1994**, *41*, 331–442; b) C. G. Pierpont, A. S. Attia, *Collect. Czech. Chem. Commun.* **2001**, *66*, 33–51; c) H. Chun, C. N. Verani, P. Chaudhuri, E. Bothe, E. Bill, T. Weyhermuller, K. Wieghardt, *Inorg. Chem.* **2001**, *40*, 4157–4166; d) P. Chaudhuri, C. N. Verani, E. Bill, E. Bothe, T. Weyhermuller, K. Wieghardt, *J. Am. Chem. Soc.* **2001**, *123*, 2213–2223; e) D. Herebian, P. Ghosh, H. Chun, E. Bothe, T. Weyhermuller, K. Wieghardt, *Eur. J. Inorg. Chem.* **2002**, 1957–1967; f) D. N. Hendrickson, C. G. Pierpont, *Top. Curr. Chem.* **2004**, *234*, 63–95.

[19] C. W. Lange, C. G. Pierpont, *J. Am. Chem. Soc.* **1992**, *114*, 6582–6583.

[20] a) B. de Bruin, E. Bill, E. Bothe, T. Weyhermüller, K. Wieghardt, *Inorg. Chem.* **2000**, *39*, 2936; b) P. H. M. Budzelaar, B. de Bruin, A. W. Gal, K. Wieghardt, J. H. van Lenthe, *Inorg. Chem.* **2001**, *40*, 4649–4655; c) D. Enright, S. Gambarotta, G. P. A. Yap, P. H. M. Budzelaar, *Angew. Chem. Int. Ed.* **2002**, *41*, 3873–3876; *Angew. Chem.* **2002**, *20*, 4029–4032; d) I. Sugiyama, I. Korobkov, S. Gambarotta, A. Mueller, P. H. M. Budzelaar, *Inorg. Chem.* **2004**, *43*, 5771–5779; e) J. Scott, S. Gambarotta, I. Korobkov, Q. Knijnenburg, B. de Bruin, P. H. M. Budzelaar, *J. Am. Chem. Soc.* **2005**, *127*, 17204–17206.

[21] T. M. Kooistra, D. G. H. Hetterscheid, E. Schwartz, Q. Knijnenburg, P. H. M. Budzelaar, A. W. Gal, *Inorg. Chim. Acta* **2004**, *357*, 2945–2952.

[22] Q. Knijnenburg, A. D. Horton, H. van der Heijden, T. M. Kooistra, D. G. H. Hetterscheid, J. M. M. Smits, B. de Bruin, P. H. M. Budzelaar, A. W. Gal, *J. Mol. Catal. A* **2005**, *232*, 151–159.

[23] T. Büttner, J. Geier, G. Frison, J. Harmer, C. Calle, A. Schweiger, H. Schönberg, H. Grützmacher, *Science* **2005**, *307*, 235–238.

[24] P. Maire, M. Königsmann, A. Sreekanth, J. Harmer, A. Schweiger, H. Grützmacher, *J. Am. Chem. Soc.* **2006**, *128*, 6578–6580.

[25] P. Maire, A. Sreekanth, T. Büttner, J. Harmer, I. Gromov, H. Rüegger, F. Breher, A. Schweiger, H. Grützmacher, *Angew. Chem. Int. Ed.* **2006**, *45*, 3265–3269; *Angew. Chem.* **2006**, *118*, 3343–3347.

[26] F. Breher, C. Böhler, G. Frison, J. Harmer, L. Liesum, A. Schweiger, H. Grützmacher, *Chem. Eur. J.* **2003**, *9*, 3859–3866.

[27] a) E. Makrtik, J. Hanzlik, A. Camus, *J. Org. Chem.* **1977**, *142*, 95; b) J. Orsini, W. E. Geiger, *J. Electroanal. Chem.* **1995**, *380*, 83; c) J. Orsini, W. E. Geiger, *Organometallics* **1999**, *18*, 1854.

[28] J. H. B. Chenier, M. Histed, J. A. Howard, H. A. Jolly, H. Morris, B. Mile, *Inorg. Chem.* **1989**, *28*, 4114.

[29] a) A. J. Kunin, E. J. Nanni, R. Eisenberg, *Inorg. Chem.* **1985**, *24*, 1852; b) G. C. Johnston, M. C. Baird, *J. Organomet. Chem.* **1986**, *314*, C51; c) B. Bogdanovic, W. Leitner, C. Six, U. Wilczok, K. Wittmann, *Angew. Chem. Int. Ed. Engl.* **1997**, *36*, 502; d) K. T. Mueller, A. J. Kunin, S. Greiner, T. Henderson, R. W. Kreilick, R. Eisenberg, *J. Am. Chem. Soc.* **1987**, *109*, 6313.

[30] B. de Bruin, J. C. Russcher, H. Grützmacher, work in progress.

[31] L. Cataldo, S. Choua, T. Berclaz, M. Geoffroy, N. Mézailles, N. Avarvari, F. Matthey, P. Le Floch, *J. Phys. Chem. A* **2002**, *106*, 3017–3022.

[32] a) E. Makrtik, J. Hanzlik, A. Camus, *J. Organomet. Chem.* **1977**, *142*, 95–103; b) J. Orsini, W. E. Geiger, *J. Electroanal. Chem.* **1995**, *380*, 83–90.

[33] M. P. García, M. V. Jiménez, L. A. Oro, F. J. Lahoz, P. J. Alonso, *Angew. Chem. Int. Ed. Engl.* **1992**, *31*, 1527–1529; *Angew. Chem.* **1992**, *104*, 1513–1514.

[34] M. P. García, M. V. Jiménez, L. A. Oro, F. J. Lahoz, J. M. Casas, P. J. Alonso, *Organometallics* **1993**, *12*, 3257–3263.

[35] a) M. J. Shaw, W. E. Geiger, J. Hyde, C. White, *Organometallics* **1998**, *17*, 5486–5491; b) M. J. Shaw, J. Hyde, C. White, W. E. Geiger, *Organometallics* **2004**, *23*, 2205–2208.

[36] R. E. Dessy, R. B. King, M. Waldrop, *J. Am. Chem. Soc.* **1966**, *88*, 471–476.

[37] R. E. Dessy, R. B. King, M. Waldrop, *J. Am. Chem. Soc.* **1966**, *88*, 5112–5117.

[38] B. de Bruin, T. P. J. Peters, S. Thewissen, A. N. J. Blok, J. B. M. Wilting, R. de Gelder, J. M. M. Smits, A. W. Gal, *Angew. Chem. Int. Ed.* **2002**, *41*, 2135–2138; *Angew. Chem.* **2002**, *114*, 2239–2242.

[39] B. de Bruin, S. Thewissen, T.-W. Yuen, T. P. J. Peters, J. M. M. Smits, A. W. Gal, *Organometallics* **2002**, *21*, 4312–4314.

[40] D. G. H. Hetterscheid, J. M. M. Smits, B. de Bruin, *Organometallics* **2004**, *23*, 4236–4246.

[41] D. G. H. Hetterscheid, B. de Bruin, J. M. M. Smits, A. W. Gal, *Organometallics* **2003**, *22*, 3022–3024.

[42] D. G. H. Hetterscheid, M. Klop, R. J. N. A. M. Kicken, J. M. M. Smits, E. J. Reijerse, B. de Bruin, *Chem. Eur. J.*, manuscript accepted.

[43] S. L. van Voorhees, B. B. Wayland, *Organometallics* **1987**, *6*, 204–206.

[44] Y. Ni, J. P. Fitzgerald, P. Carrol, B. B. Wayland, *Inorg. Chem.* **1994**, *33*, 2029–2035.

[45] M. Wei, B. B. Wayland, *Organometallics* **1996**, *15*, 4681–4683.

[46] D. G. DeWitt, *Coord. Chem. Rev.* **1996**, *147*, 209–246.

[47] J. E. Anderson, C.-L. Yao, K. M. Kadish, *Inorg. Chem.* **1986**, *25*, 718–719.

[48] J. E. Anderson, C.-L. Yao, K. M. Kadish, *Organometallics* **1987**, *6*, 706–711.

[49] J. E. Anderson, C.-L. Yao, K. M. Kadish, *J. Am. Chem. Soc.* **1987**, *109*, 1106–1111.

[50] B. B. Wayland, *Polyhedron* **1988**, *16*/*17*, 1545–1555.

[51] B. B. Wayland, S. Ba, A. E. Sherry, *J. Am. Chem. Soc.* **1991**, *119*, 5305–5311.

[52] B. B. Wayland, V. L. K. Coffin, M. D. Farnos, *Inorg. Chem.* **1988**, *27*, 2745–2747.

[53] B. B. Wayland, A. E. Sherry, A. G. Bunn, *J. Am. Chem. Soc.* **1993**, *115*, 7675–7684.

[54] L. Basickes, A. W. Bunn, B. B. Wayland, *Can. J. Chem.* **2001**, *79*, 854–856.

[55] H. Zhai, A. Bunn, B. B. Wayland, *Chem. Commun.* **2001**, 1294–1295.

 © 2007 Wiley-VCH Verlag GmbH & Co. KGaA, Weinheim

[56] R. S. Paonessa, N. C. Thomas, J. Halpern, *J. Am. Chem. Soc.* **1985**, *107*, 4333–4335.
[57] B. B. Wayland, G. Poszmik, M. Fryd, *Organometallics* **1992**, *11*, 3534–3542.
[58] H. Ogoshi, J. Setsunu, Z. Yoshida, *J. Am. Chem. Soc.* **1977**, *99:11*, 3869–3870.
[59] B. B. Wayland, A. E. Sherry, G. Pozmik, A. G. Bunn, *J. Am. Chem. Soc.* **1992**, *114*, 1673–1681.
[60] A. G. Bunn, B. B. Wayland, *J. Am. Chem. Soc.* **1992**, *114*, 6917–6919.
[61] L. Brammer, N. G. Connelly, J. Edwin, W. E. Geiger, A. G. Orpen, J. B. Sheridan, *Organometallics* **1988**, *7*, 1259–1265.
[62] B. B. Wayland, A. E. Sherry, A. G. Bunn, *J. Am. Chem. Soc.* **1993**, *115*, 7675–7684.
[63] L. Basickes, A. W. Bunn, B. B. Wayland, *Can. J. Chem.* **2001**, *79*, 854–856.
[64] H. Zhai, A. Bunn, B. B. Wayland, *Chem. Commun.* **2001**, 1294–1295.
[65] X.-X. Zhang, G. F. Parks, B. B. Wayland, *J. Am. Chem. Soc.* **1997**, *119*, 7938–7944.
[66] B. B. Wayland, K. J. Del Rossi, *J. Organomet. Chem.* **1984**, *276*, C27–C30.
[67] M. S. Sanford, J. T. Groves, *Angew. Chem. Int. Ed.* **2004**, *43*, 588–590; *Angew. Chem.* **2004**, *116*/*5*, 598–600.
[68] M. Feng, K. S. Chan, *J. Organomet. Chem.* **1999**, *584*, 235–239.
[69] K. W. Mak, S. K. Yeung, K. S. Chan, *Organometallics* **2002**, *21*, 2362–2364.
[70] M. K. Tse, K. S. Chan, *J. Chem. Soc., Dalton Trans.* **2001**, 510–511.
[71] S. K. Yeung, K. S. Chan, *Organometallics* **2005**, *24*, 6426–6430.
[72] B. B. Wayland, Y. Feng, S. Ba, *Organometallics* **1989**, *8*, 1438–1441.
[73] A. D. Burrows, M. Green, J. C. Jeffery, J. M. Lynam, M. F. Mahon, *Angew. Chem. Int. Ed.* **1999**, *38*, 3043–3045; *Angew. Chem.* **1999**, *111*, 3228–3230.
[74] B. de Bruin, P. H. M. Budzelaar, A. W. Gal, *Angew. Chem. Int. Ed.* **2004**, *43*/*32*, 4142–4157; *Angew. Chem.* **2004**, *116*, 4236–4251, and references therein.
[75] C. Tejel, M. A. Cireano, *Top. Organomet. Chem.*, accepted.
[76] R. J. N. A. M. Kicken, PhD Thesis, University of Nijmegen, **2001**.
[77] B. de Bruin, J. A. Brands, J. J. J. M. Donners, M. P. J. Donners, R. de Gelder, J. M. M. Smits, A. W. Gal, *Chem. Eur. J.* **1999**, *5*, 2921.
[78] B. de Bruin, unpublished results.
[79] D. G. H. Hetterscheid, B. de Bruin, *J. Mol. Catal. A* **2006**, *251*, 291–296.
[80] For examples see the NIEST spin-trap database, which can be found at: https://dir-apps.niehs.nih.gov/stdb/index.cfm. Supporting references are provided therein.
[81] a) L. Carlton, G. Read, M. Urgelles, *J. Chem. Soc., Chem. Commun.* **1983**, 586; b) J. M. Takacs, X.-T. Jiang, *Curr. Org. Chem.* **2003**, *7*, 369.
[82] a) E. Donato, F. C. Priolo, *J. Organomet. Chem.* **1983**, *251*, 273; b) D. A. White, *J. Chem. Soc. A* **1971**, 145; c) J. K. Stille, D. E. James, *J. Am. Chem. Soc.* **1975**, *97*, 674.
[83] See for example: H. M. L. Davies, R. E. J. Beckwith, *Chem. Rev.* **2003**, *103*, 2861–2903 and references cited therein.
[84] J. R. Krumper, M. Gerisch, J. M. Suh, R. G. Bergman, T. D. Tilley, *J. Org. Chem.* **2003**, *68*, 9705–9710.
[85] D. G. H. Hetterscheid, C. Hendriksen, W. I. Dzik, J. M. M. Smits, E. R. H. van Eck, A. E. Rowan, V. Busico, M. Vacatello, V. Van Axel Castelli, A. Segre, E. Jellema, T. G. Bloemberg, B. de Bruin, *J. Am. Chem. Soc.* **2006**, *128*, 9746–9752.

Received: September 29, 2006
Published Online: December 11, 2006

 © 2007 Wiley-VCH Verlag GmbH & Co. KGaA, Weinheim